DISSERTATION

A Numerical Scheme for the Hele-Shaw Problem in Oscillating Media

Graduate School of Natural
Sciences And Technology
Kanazawa University

Division of Mathematical
and Physical Sciences

Student ID No. : **1524012011**
Name : **Irma Palupi**
Chief Advisor : Prof. **Seiro Omata**
Date of Submission : June 29, 2018

Abstract

We study the Hele-Shaw problem in oscillating media, and mainly are interested in the averaging behavior of the free boundary velocity, that is a homogenization problem. Our focus is only on the one-phase Hele-Shaw problem neglecting the surface tension. A general formula for the homogenized velocity is unknown. Current results are known for the media periodic only in space or only in time. In this work, we develop an efficient numerical scheme to estimate the averaging velocity in two dimensions with periodic coefficients in both space and time. Also for comparison, we implement the regular finite difference to obtain a numerical solution and we describe how to get a free boundary position. We present several computation experiments to test the error of both for the numerical solution and the free boundary position.

Acknowledgements

I would like to express my sincere gratitude for my chief supervisor, Professor Seiro Omata for his continuous support during my study at Kanazawa University. I also would like to express my deep gratitude to Assistant Professor Norbert Požár for his patience and guidance during my research work. I thank for every opportunity to learn at Kanazawa University, to join the interesting courses and to attend the special lectures held by Department of Mathematical and Physical Sciences which give me a new sight for the field that I am interested in. I also thank the doctoral program for the development of Global Human Resources in Mathematical and Physical Sciences (GHR program) with support from Ministry of Education, Culture, Sports, Science, and Technology (MEXT) for the generous opportunity to be part of the program. My Deep appreciation is also for all members of Omata laboratory and Japan Indonesian Student Community (PPI) in Kanazawa for their help and the life suggestions, especially at the beginning of living in this town. Finally, I wish to thank my parents for their love, supports, and encouragements in my entire life. Thank you for never giving up to strengthen me to believe.

Contents

List of Figures

Abbreviations

HS	**H**ele **S**haw
SF	**S**te**f**an Problem
BBR	**B**erger **B**rézis **R**ogers
SOR	**S**uccessive **O**ver**R**elaxation

Chapter 1

Introduction

1.1 Introduction

Patterns in nature have been of interest for many years in various fields of science. They appear in numerous natural phenomena that have an order or repeated systematic structure. Scientists want to capture them in their models to understand the rules of their formulation. Interestingly, different natural phenomena may have similar pattern. For instance, the pattern in branching of a tree look similar to the ice crystallization, dendritic copper, and the burned wet pine if the electricity is run between two nails sunk into it, and also to the flow of viscous fluid.

Particularly in the fluid mechanics, researches studying a pattern of a flow in order to learn various of its behavior, such as abnormality, direction, strength, etc. In fluids, the patterns are usually caused by instabilities. For example in the interaction of two fluids, Rayleigh-Taylor instability shows a mushroom-like pattern as an indication of mixing two different densities of the fluids. There is also an instability caused by the difference between tangential velocities of fluids that shows as a triangle-wave pattern forms a cloud-like shape. The example study of such instabilities can be found in the Saffman-Taylor instability. They

discovered a finger-like pattern on the interface in between fluids with different viscosities, called *viscous fingering*. They observed such a pattern in the porous medium and Hele-shaw cell [1]. Hele-Shaw cell is an experiment invented by Henry Selby Hele-Shaw. It presents a fluid flow through a narrow gap between parallel plates, which for many years was used as a model to approximate various problems of viscous fluid in fluid mechanics.

Furthermore, a pattern occurs in two different types of geometry, radial and rectangular. Viscous fingering in a rectangular geometry refers to the Hele-Shaw cell with a less viscous fluid injected continuously from one end of the cell. In this situation, the interface is transported by the gradient of pressure (sufficiently high) through a more viscous area and an instability occurs which forms a finger-like pattern on the interface. The interface is initially flat. Once the pressure drives to the more viscous part, the interface starts to show a single finger where the gradient is locally highest at the tip. After some time the tip will turn blunt, then split into a branch of fingers. Each finger on the branch growths independently.

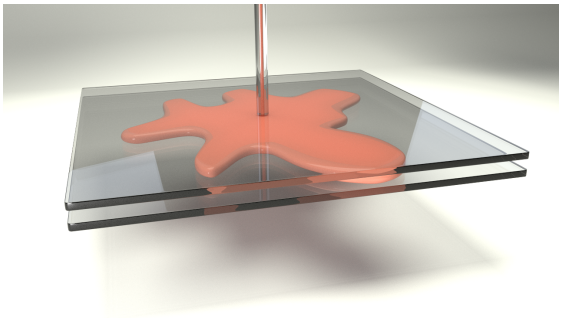

FIGURE 1.1: Hele-Shaw cell experiment (Pozar, 2018. Used with permission.).

On the other hand, radial viscous fingering occurs when injecting a Hele-Shaw cell through a source point in the middle of the plates. Initially, the interface is given by a circle, then it spreads and splits turning into radial fingering pattern. Unlike in the rectangular fingering, there is no such single finger appearance in radial geometry. Once the interface becomes unstable, it will turn into radial fingering-look. This pattern also looks familiar with a typical pattern in bacteria

growth, crystal growth, and tumor growth for instance. Hele-shaw problem appears in many fields area. It is an example of non-linear diffusion phenomena. Many industry fields implement the Hele-shaw model to approximate the real situation in their sector, for example, a molding process in the plastic industry [2], petroleum extraction in the oil industry, and many other examples.

In many years, Hele-Shaw problems have been one of popular model in fluid mechanics. Researchers in porous media and the flow in between two parallel plates consider this problem as a reliable model. In this work, we study the Hele-Shaw problem in oscillating media, and mainly are interested in the averaging behavior of the free boundary velocity, namely the homogenization problem. Our focus is only on the one-phase Hele-Shaw problem neglecting surface tension.

One can merely represent this problem as a flow of a liquid through the valleys area, and we are interested in the homogenized behavior of the free boundary. For a general type of media, the homogenized solution for Hele-Shaw is unknown. Current results know only for the media that periodic only in space or only in time [3]. We recently developed a numerical scheme to estimate the homogenized normal velocity in the Hele-Shaw problem with periodic coefficients in both space and time, see [4].

The homogenization method has many important practical implementations in material sciences since the macroscopic appearance are mostly used in industry. It comes from the fact that the macroscopic appearance has better characteristics in a practical industry than the microscopic point of view. In the microscopic appearance, there will appear the heterogeneities that become a source of error such that computationally it is difficult to be implemented. Therefore the theory of homogenization which describes the behavior of a composite material from the local characteristics of the heterogeneities answering the difficulties.

Instead of directly solving the problem, using the fact that the Hele-Shaw problem can be described as the zero specific heat limit of the one-phase Stefan problem, we consider a Stefan problem in enthalpy formulation to solve the problem. Since the Stefan equation is a nonlinear equation, we must find a method that reduces the nonlinearity so that we perform the computation significantly faster than the explicit finite difference scheme. We use the method firstly developed by Berger, Brézis, and Rogers in [5] to solve a similar nonlinear homogeneous problem. We will refer to it as the BBR method. As it uses an implicit scheme, it is also essential to choose an efficient numerical method to solve the implicit scheme. It turns out that a multigrid scheme for the linear elliptic problem works well even though there is a jump across the free boundary.

1.2 Content of the thesis

We are interested in developing a numerical method to efficiently compute the numerical solution of Hele-Shaw problem for both Dirichlet and Neumann boundary data. Furthermore, we apply the method to approximate a numerical solution of a homogenized problem of a given media that are periodic both in space and time, and moreover to observe the homogenized velocity in such periodic media. The content of the thesis is as follows. In chapter 2, we brief the formulation of the governing equation for the Hele-shaw problem and the homogenization problem. We explain current results for averaging free boundary velocity if the media depends only on time or only on space. The idea to approximate the average normal velocity for general direction in 2D is adapted from the one specific direction case only. In chapter 3, we explain the consideration of indirectly solving the Hele-Shaw problem via the Stefan problem in the enthalpy formulation. Here, we consider two problems, the problem with source spreading from the middle of the area of the plate (Dirichlet boundary data), and a Neumann problem. In chapter 4,

explicit finite difference scheme is explained to obtain a numerical solution in both one dimension and two dimensions, especially how to approximate the free boundary. We also make several observations of the numerical solution. In chapter 5, we explain the advanced implicit method to solve the equation in the enthalpy form, which we call the BBR scheme. In chapter 6, we describe how does the Multigrid linear solver is adapted to our problem. Finally, in chapter 7, we give the implementation of the BBR scheme to estimate the free boundary velocity in two dimensions. Several interesting results are shown in this chapter.

Chapter 2

Hele-Shaw Problem

2.1 Physical Phenomena

In two dimensional case, Hele-shaw problem is a two dimensional model for the pressure-driven flow of viscous liquid throughout a very tiny gap of two plates with given boundary data on the source. This model has several applications, such as in electro-machining, injection molding, and even basic model for tumor growth, and many other industrial fields. Furthermore, in three-dimensional model Hele-Shaw problem appears in the porous medium, i.g pipe injection in the petroleum field. In the plastic molding process, in particular, it is useful to determine the end position of the melting plastic will be filling the mold, which is the circulation hole for the air to way out.

There are several more specific problem refer to this model. One-phase Hele-Shaw problem is usually describing the evolution of a liquid being injected into a Hele-shaw cell, and the free boundary problem occurs on the liquid surface against the air. Meanwhile, a two-phase Hele-shaw problem can be a model for free boundary problem of two liquids having a different viscosity. In three dimensional case, this model refers to the problem called porous medium equation. However, in this

research work, our interest is in the one-phase Hele-shaw problem in two dimensions with neglecting the effect of surface tension on the boundary.

2.1.1 Governing Equation for Hele-Shaw Flow

This work focus only on the scope of the Newtonian fluid. In fluid dynamics, Hele-Shaw flow is one of Stokes flow of a liquid that distributes through a very tiny space between two plates which continually injected by fluid from the source inside the fluid area. This phenomenon can be derived from conservation law of mass, where saying that a density changing per unit volume depend only on the flux passing through its boundary, either due to the absence of fluid transport or due to volume movement, and a given external source. It states that changing a mass

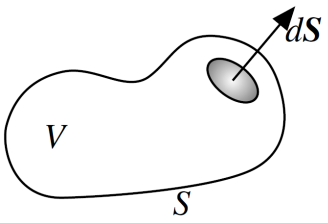

in the fixed domain V is proportional to a given flux q moves to the boundary of V in the normal direction, and a given external source contribution $f(x,t)$.

$$\begin{aligned}\frac{d}{dt}\int_V \rho dV &= \int_S q \cdot dS + \int_V f(x,t)dV \\ &= \int_V \nabla \cdot q dV + \int_V f(x,t)dV \text{ , by divergent theorem} \\ &\Leftrightarrow \rho_t - \nabla \cdot (q) = f(x,t) \text{ ,since fixed volume V.}\end{aligned} \tag{2.1.1}$$

Since the flux is caused by the difference of pressure u, $q = -\rho\nabla u$ and no outer source, then from the we obtain,

$$\rho_t + \nabla(\rho\nabla u) = 0. \tag{2.1.2}$$

We assume that the liquid is an incompressible fluid (e.g water), therefore it remains the following Laplace equation.

$$\Delta u = 0 \tag{2.1.3}$$

In a Hele-Shaw cell, we consider the flow of a Newtonian viscous fluid that is incompressible, and driven by pressure caused by a constant given source in the middle of the cell. Hele-shaw problem can be derived from the equation for the motion of viscous fluid, i.e Navier-Stokes equation with neglecting the external body force. Suppose that Ω_t be the diffuse region in coordinate (x, y) of a liquid at time t and $2h$ is a length of gap between the plates. Outside of diffuse region is filled only by the air and we assume has zero pressure $u = 0$. For $h \to 0$, the velocity in the vertical direction z is parabolic and determining the constants so as to make the velocity $q = 0$ at $z = \pm h$, so that it satisfies

$$q = -\frac{1}{2\mu}(h^2 - z^2)\nabla u \tag{2.1.4}$$

where μ is a fluid viscosity, such that the average of velocity over the gap is following

$$\bar{q} = \frac{1}{2h}\int_{-h}^{h} q dz = -\frac{h^2}{12\mu}\nabla u. \tag{2.1.5}$$

The average velocity $\bar{q}$ also satisfies the continue equation in 2D, such that it implies that the pressure u in Ω_t satisfies Laplace equation

$$\Delta u = 0.$$

For the boundary condition on the free boundary $\partial\Omega_t$, there are dynamic and kinetic boundary condition. The dynamic boundary condition occurs to be

$$u = 0 \qquad \text{on } \partial\Omega_t,$$

since we neglecting the surface tension. And for the kinematic boundary condition, the normal velocity of the fluid particles on the boundary satisfying

$$V_n = \bar{q} \cdot \nu \qquad \text{on } \partial\Omega_t \tag{2.1.6}$$

where ν is the unit outer normal vector on $\partial\Omega_t$. Since u can be seen as a level set, (2.1.6) can be rewritten as

$$V_n = -k|\nabla u| = \frac{u_t}{|\nabla u|} \tag{2.1.7}$$

where k is a constant equals to $-\frac{h^2}{12\mu}$.

2.1.2 Hele-shaw Problem as a limit of Stefan Problem

Suppose the Hele-Shaw problem is in $\mathbb{R}^n$, $n = 2$. Given Ω_0 as an initial domain for given initial data u_0, and $K \subset \Omega_0 \subset \Omega_t,\ t > 0$ be a closed subset. We want to find a pair of $u(x,t)$ and free boundary $\partial\Omega_t$ that satisfying (HS).

$$\begin{cases} \Delta u(x,t) = 0 & \text{for } (x,t) \in (\Omega_t \setminus K) \times (0,\infty) \\ u_t = g(x,t)|\nabla u|^2, & \text{for}(x,t) \in \partial\Omega_t \times (0,\infty) \\ u(x,t) = 1 & \text{for}(x,t) \in K \times (0,\infty) \\ u(x,t) = 0 & \text{for}(x,t) \in \overline{(\mathbb{R}^n \setminus \Omega_t)} \times (0,\infty) \end{cases} \tag{HS}$$

Solution $u(x,t)$ represents the pressure of some viscous fluid that is injected into Hele-shaw cell. The area with no fluid is assumed to have zero pressure, and function $g(x,t)$ is a given continuous positive function, denoting media representation. As in the original Hele-shaw problem, this function is some constant k which describing a homogeneous structure of the media. $\frac{1}{g}$ can be representing a depth of the hole

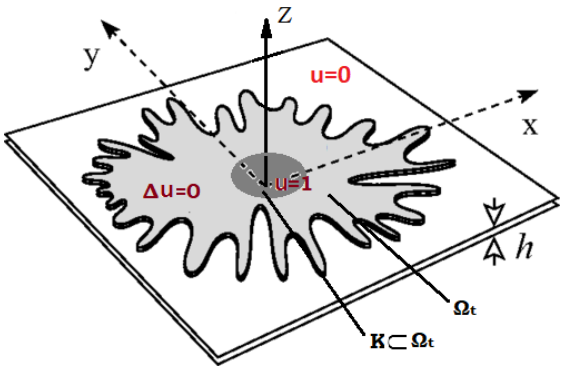

FIGURE 2.1: Hele-Shaw cell for problem (HS)

must be filled by a liquid when evolving. This value change in the position and time.

If we look at the one-phase Stefan problem, the free boundary problem is similar except on the term first time derivative in the Stefan problem. The heat diffusion speed depends on the heat specific parameter c (see chapter 3), that is the quantity of heat required to change the temperature 1 degree celsius in one unit of mass. As $c \to 0$ the Stefan problem approaches the Hele-shaw problem, and as $t \to \infty$ the temperature diffusion will reach the steady-state and no longer has the term first-time derivative. The work in [6] explains the asymptotic behavior of the solutions between two problems including the free boundaries as $t \to \infty$. They explain the behavior in the aspect of the near-field limit and far-field limit. It states for 1 dimensional case when $g(x,t)$ is constant both in x and t, the self-similar solution of two problems converge to the same constant as $t \to \infty$ for every $x > 0$. The convergence is not uniform. Despite the free boundary of both problem have the same growth rate $\sqrt{t}$, the free boundary of the 1-D Stefan problem converge to Hele-Shaw when $c \to 0$.

Different to the 1-D case, The solution of Stefan problem is not ultimately to be the Hele-shaw as $t \to \infty$, for $n >= 2$ there is only the convergence behavior to a stationary state of both problem, and the asymptotic behavior is different. Meanwhile, in 2 dimensions case, it shows that the Stefan problem simplifies to

the Hele-shaw. An unlikely 1-D case, the HS and SF problem for multidimensional spaces do not always have a classical solution. However, they always have a weak solution globally over time.

2.2 Homogenized Hele-Shaw Problem

Homogenization theory is concerned with the effects of rapidly varying coefficients to the solution of PDE. This problem appears in obtaining the macroscopic equation for the system with a fine microscopic structure for instance, which is to be our interest. Suppose that we have two different length scale of oscillation period in PDE respectively for macroscopic and microscopic structure, 1 and $0 < \epsilon < 1$. For fixed ϵ we have a solution u^ϵ for microscopic scale and u for the macroscopic, are different and complicated in general. Homogenization theory studies the limiting behavior of the solution of microscopic to the homogenized problem as $\epsilon \to 0$. The idea is the limit effects toward homogenized problem will be the averaged out of the fine-structure.

For example in a periodic homogenization of elliptic problem, we have quantity u satisfying the elliptic equation

$$-\nabla \cdot (A(x)\nabla u(x)) = f(x). \tag{2.2.1}$$

The microscopic solution u^ϵ for fixed oscillation period ϵ satisfies

$$-\nabla \cdot (A(\frac{x}{\epsilon})\nabla u^\epsilon(x)) = f(x). \tag{2.2.2}$$

As $\epsilon \to 0$, we have $u^\epsilon \to u^h$, where u^h is solution satisfied the homogenized form

$$-\nabla \cdot (A^h \nabla u^h). \tag{2.2.3}$$

Thus, homogenization problem are to find the asymptotic convergence of solution $u^\epsilon \to u^h$, and to obtain the expression for A^h which is not simply the average of $A(\frac{x}{\epsilon})$ in general.

However, for the Hele-shaw problem we are interested in the convergence as $\epsilon \to 0$ of the solution u^ϵ, and the structure of homogenized free boundary velocity. In the work of [7], they derive the explicit formula for homogenized free boundary velocity with function $g = g(x)$ depends only on space variable, and establish the uniform convergence of the free boundary. Furthermore, [3] consider the homogenization in heterogeneous media both in space and time, and found that the free boundaries for various dependence of normal velocity converge locally uniformly in Hausdorff distance. It was also observed that non-periodic, fractal-like variations in the flow lead to anomalous diffusion in Stefan and Hele-Shaw problems [8].

2.2.1 Homogenized Hele-Shaw Problem

Suppose that the Hele-shaw cell in the periodic media is given by the problem to find $u = u(x,t)$, $\Omega \subset \mathbb{R}^n \times [0,\infty)$, $(\Omega(t) : \{x|(x,t) \in \Omega\})$ such that:

$$\begin{cases} \Delta u(\cdot,t) = 0 & \text{in } \Omega(t) \setminus K, t > 0 \\ V(x,t) = g(\frac{x}{\epsilon}, \frac{t}{\epsilon})|\nabla u(x,t)| & x \in \partial\Omega(t), t > 0 \\ \Omega(0) = \Omega_0 & \\ u = h & \text{on } K \\ u = 0 & \text{on } \partial\Omega(t), t > 0 \end{cases} \tag{2.2.4}$$

for given $h > 0$, and $g > 0$ 1-periodic function $(g(x+k,t+l) = g(x,t), k \in \mathbb{Z}^N, l \in \mathbb{Z}^N)$.

and for scale $\varepsilon > 0$ we introduce the rescaled $g^\varepsilon(x,t) := g(\frac{x}{\varepsilon}, \frac{t}{\varepsilon})$. Note that in general scaling $g(\varepsilon^\alpha x, \varepsilon^\beta t)$ is possible, but it leads to a simpler behavior than this critical scaling $\alpha = \beta$, see for example [9]. Keeping all other parameters fixed, for every given $\varepsilon > 0$ we get a solution $\{\Omega_t^\varepsilon\}_{t\geq 0}$, u^ε of (2.2.4) with $g = g^\varepsilon$. The goal is to identify the homogenization limit $\varepsilon \to 0$ of these solutions.

We shall denote

$$\Omega = \bigcup_{t\geq 0} \Omega_t \times \{t\} \quad \text{and} \quad \Omega^\varepsilon := \bigcup_{t\geq 0} \Omega_t^\varepsilon \times \{t\}.$$

In [3], under certain regularity assumptions on the data K, Ω_0 and g, it was proved that there exist limits $\{\Omega_t\}_{t\geq 0}$ and u such that $u^\varepsilon \to u$ in the sense of half-relaxed limits and $\partial\Omega^\varepsilon \to \partial\Omega$ in Hausdorff distance. Furthermore, the pair (Ω, u) is the unique solution of the *homogenized problem* in which Ω evolves with the normal free boundary velocity

$$V = r(\nabla u) \qquad x \in \partial\Omega_t \tag{2.2.5}$$

and u is again the solution of (HS), where $r : \mathbb{R}^n \to \mathbb{R}$ is a nonnegative function that depends only on g.

A straightforward modification of the arguments in [3] shows the same homogenization result if the Dirichlet boundary condition on ∂K in (HS) is replaced by a Neumann boundary condition $\frac{\partial u}{\partial \nu}(\cdot, t) = 1$.

However, there does not seem to be any explicit formula for $r(q)$, and it is not even known whether r is continuous in general. It is only known that $r^*(a_1 q) \leq r_*(a_2 q)$ for any $0 < a_1 < a_2$ and any $q \in \mathbb{R}^n \setminus \{0\}$, where r^* and r_* denote the upper and lower semicontinuous envelopes of r, respectively. See [3] for more details. Formal calculations indicate that $r(q)$ is in general only $\frac{1}{2}$-Hölder continuous if g is smooth and $r(q)$ might be discontinuous if g is only Hölder [10]. Our goal is to estimate

$r(q)$ *numerically*. We are in particular interested whether the homogenized problem has solutions whose free boundary develops flat parts (*facets*).

2.2.2 Homogenized Problem in 1-D

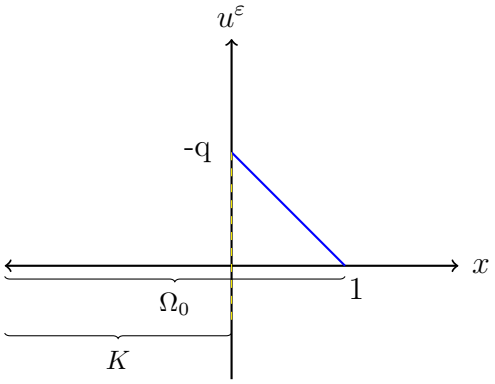

Let $K = (-\infty, 0]$ and $\Omega_0 = (-\infty, 1)$, and we use the boundary condition $u_x(0,t) = q$ on $\partial K = \{0\}$ for some $q < 0$ in (HS). Then $\Omega_t^\varepsilon = (-\infty, y^\varepsilon(t))$ for some $y^\varepsilon > 0$. The solution of Laplace's equation is $u^\varepsilon(x,t) = q(x - y^\varepsilon(t))$ in this case. The free boundary velocity equation for Ω^ε simplifies to

$$\begin{cases} (y^\varepsilon)'(t) = g(\frac{y^\varepsilon(t)}{\varepsilon}, \frac{t}{\varepsilon})|q|, \quad t > 0, \\ y^\varepsilon(0) = 1, \end{cases} \tag{2.2.6}$$

which is a simple initial-value problem for an ordinary differential equation (ODE). It is known, see [9, 11], that y^ε converges locally uniformly as $\varepsilon \to 0+$ to the solution y of the ODE

$$\begin{cases} y'(t) = r(q), \quad t > 0, \\ y(0) = y_0, \end{cases}$$

where $r : \mathbb{R} \to \mathbb{R}$ depends only on g. This equation has the unique solution $y(t) = y_0 + tr(q)$. We can therefore *estimate* $r(q)$ *numerically* by solving (2.2.6)

for a small $\varepsilon > 0$ and finding

$$r(q) = y(1) - y_0 \approx y^\varepsilon(1) - y_0.$$

By a scaling argument, this can be shown equivalent to solving (2.2.6) with $\varepsilon = 1$ for a large time $T \gg 1$ and then finding

$$r(q) = \frac{y(T) - y_0}{T} \approx \frac{y^1(T) - y_0}{T}.$$

Since (2.2.6) can be efficiently solved numerically, we can estimate $r(q)$ rather easily.

The actual form of $r(q)$ is known only in certain cases [9]:

- $g(x,t) = g(t)$: if g depends only on t, then $r(q) = \langle g \rangle q$, where $\langle g \rangle = \int_0^1 g(t)\, dt$ is the average of g.
- $g(x,t) = g(x)$: if g depends only on x, then $r(q) = \frac{1}{\left\langle \frac{1}{g} \right\rangle} q$, where $\left\langle \frac{1}{g} \right\rangle = \int_0^1 \frac{1}{g(x)}\, dx$ is the average of $\frac{1}{g}$.

If g depends on both x and t nontrivially, the explicit form of $r(q)$ is not known and in fact it can be very complicated, see Figure 2.2 for an example. The number $r(q)$ is related to Poincaré's rotation number.

Nonetheless, we can still find the value of $r(q)$ at least for particular q. Particularly interesting is the existence of intervals of constant velocity, which we call *pinning intervals*. See also [10] for a related problem on a droplet motion.

Lemma 2.2.1. *Suppose that $g(x,t) = f(x-t)$ where $f = f(x)$ is a positive periodic continuous function. Then $r(q) = 1$ for $q \in [-\frac{1}{\min f}, -\frac{1}{\max f}]$.*

Proof. Let $L > 0$ be a period of f. Fix $q \in [-\frac{1}{\min f}, -\frac{1}{\max f}]$. Since $\frac{1}{|q|} \in [\min f, \max f]$, there exists $\xi \in \mathbb{R}$ such that $f(x_0) = \frac{1}{|q|}$ for all $x_0 \in \xi + L\mathbb{Z}$.

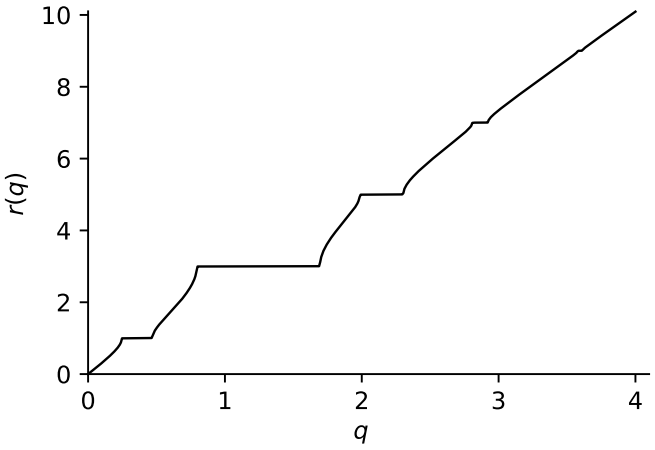

FIGURE 2.2: Sample $r(q)$ in one dimension for $g(x,t) = \sin(2\pi(x+t))+\sin(2\pi(x+3t))+3$. Note the pinning intervals at speeds $2k-1$ for $k = 1, 2, \ldots, 5$.

But $y^\varepsilon(t) = \varepsilon x_0 + t$ is then a solution of (2.2.6) for any $x_0 \in \xi + L\mathbb{Z}$ and $\varepsilon > 0$. By uniqueness of (2.2.6) (comparison principle), we conclude that $\frac{y^\varepsilon(T)-y^\varepsilon(0)}{T} = 1$ for any $\varepsilon > 0$ and therefore $r(q) = 1$. □

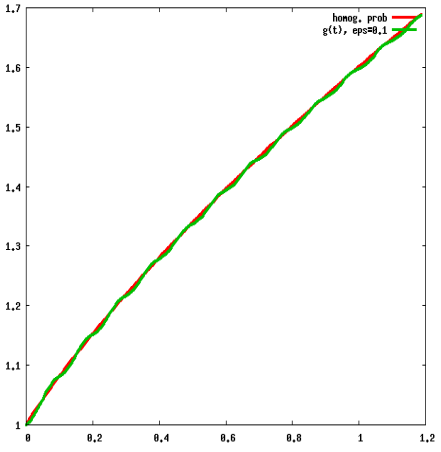

FIGURE 2.3: Free boundary position of homogenized problem with $g(x,t) = g(t)$.

2.3 Homogenization in 2-D

The shape of the free boundary $\partial\Omega^\varepsilon$ is in general not simple in two dimensions and therefore the solution of (HS) is not a linear function anymore. We therefore have

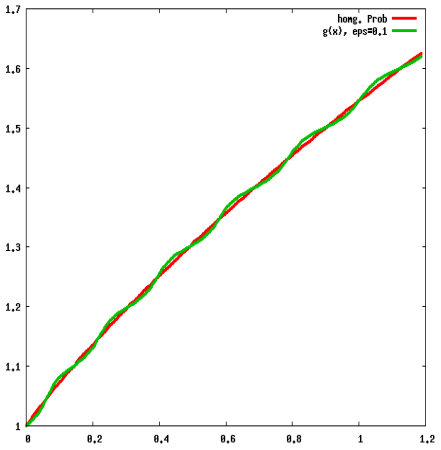

FIGURE 2.4: Free boundary position of homogenized problem with $g(x,t) = g(x)$.

to solve the full problem to estimate $r(q)$. We first observe that for a given $q \in \mathbb{R}^n$ the moving plane

$$P_q(x,t) := |q| \left(r(q)t - x \cdot \frac{q}{|q|} \right) \qquad x \in \mathbb{R}^n, t \in \mathbb{R},$$
$$\Omega_{q,t} := \{x : P_q(x,t) > 0\} = \left\{ x : x \cdot \frac{q}{|q|} < r(q)t \right\}$$

is a solution of the homogenized problem (2.2.5).

Let us suppose that $q = (q_1, 0)$ for some $q_1 < 0$. We consider the Hele-Shaw problem with $K := (-\infty, 0] \times \mathbb{R} \subset \Omega_0 := (-\infty, L_0) \times \mathbb{R} \subset \mathbb{R}^2$ for some fixed $L_0 > 0$, with Neumann boundary condition $u_{x_1}(0, x_2) = q_1$ for all $x_2 \in \mathbb{R}$. Clearly, $\Omega_{q,t} + L_0(e_1, 0)$, $P_q(\cdot - L_0 e_1, \cdot)$ is a solution of the homogenized problem in this setting. Let Ω^ε, u^ε be the solution of the ε-problem with the same boundary and initial data. By [3], we know that $\partial\Omega^\varepsilon \to \partial\Omega_q + L_0(e_1, 0)$ in Hausdorff distance. Let us fix $L_1 > L_0$ and define the first time the free boundary of the solution of the ε-problem touches the set $\{x_1 = L_1\}$,

$$T_\varepsilon := \sup \{t > 0 : \Omega_t^\varepsilon \cap \{x_1 = L_1\} = \emptyset\}.$$

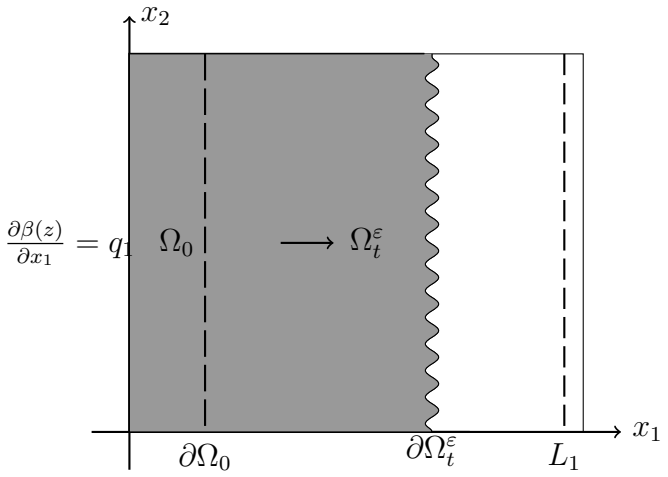

FIGURE 2.5: Neumann problem (6.1.1) in 2D case to estimate the value of $r(q)$.

By the convergence in the Hausdorff distance, we see that $T_\varepsilon \to \frac{L_1 - L_0}{r(q)}$ as $\varepsilon \to 0$. This allows us to estimate $r(q)$ by choosing $0 < \varepsilon \ll 1$ and using

$$r(q) \approx \frac{L_1 - L_0}{T_\varepsilon}.$$

We will find T_ε numerically by solving the problem on a bounded domain. To this end, we observe that if $\varepsilon = \frac{1}{\omega}$ for some $\omega \in \mathbb{N}$ sufficiently large, the uniqueness of solutions of the ε-problem implies that Ω^ε, u^ε are 1-periodic in the x_2-direction, that is, $\Omega^\varepsilon + (e_2, 0) = \Omega^\varepsilon$, $u^\varepsilon(x + e_2, t) = u^\varepsilon(x)$.

Therefore we introduce the numerical domain $U = (0,1)^2$ and solve the Hele-Shaw problem on U with boundary conditions

$$\begin{aligned}
\Omega^\varepsilon + (e_2, 0) &= \Omega^\varepsilon, \\
u_{x_1}(0, x_2, t) &= q_1 && 0 \le x_2 \le 1, t \ge 0, \\
u(x_1, x_2 + 1, t) &= u(x_1, x_2, t) && x \in \Omega_t^\varepsilon, t \ge 0,
\end{aligned}$$

see Figure 2.5.

There are direct methods to solve the Hele-Shaw problem, however, for simplicity

and efficiency, we use the fact that the solution of the Hele-Shaw problem can be in the limit $c \to 0$ approximated [12, 13] by the solution of the Stefan problem

$$\begin{cases} cu_t - \Delta u = 0 & \text{in } \Omega, \\ V = g^\varepsilon |Du| & \text{on } \partial\Omega, \end{cases} \tag{2.3.1}$$

with initial condition $u(\cdot, 0) = u_0$, where u_0 is the 1-periodic-in-x_2 solution of

$$\begin{cases} -\Delta u_0 = 0 & \text{in } \Omega_0 \setminus K \\ u_0 = 0 & \text{on } \partial\Omega_0, \\ \partial_{x_2} u_0 = q_1 & \text{on } \{x_2 = 0\}. \end{cases}$$

This problem can be rewritten in the *enthalpy* formulation by introducing $\beta(s) := \max(s, 0)$ and solving formally for $z : \mathbb{R}^n \times \mathbb{R} \to \mathbb{R}$ the solution of

$$\begin{cases} cz_t - \Delta\beta(z) = -\left(\dfrac{\partial}{\partial t}\dfrac{1}{g^\varepsilon}\right)\chi_{\text{int}\,\{z<0\}} & \text{in } U \times (0,\infty), \\ \dfrac{\partial\beta(z)}{\partial x_1}(0, x_2, t) = q_1 & x_2 \in [0,1], t > 0, \\ z \quad \text{1-periodic in } x_2, \\ z(\cdot, 0) = u_0\chi_{\Omega_0} - \dfrac{1}{cg^\varepsilon(\cdot, 0)}\chi_{\Omega_0^\complement} & \text{in } U, \end{cases} \tag{2.3.2}$$

where the first equation is understood in the sense of distributions. We can recover u as $\beta(z)$ and Ω as $\{z > 0\}$.

If $g^\varepsilon = g^\varepsilon(x)$, the well-posedness of problem (2.3.2) is well known from the theory of variational obstacle problems, see for example [14], [15], and $u = \beta(z)$ is continuous [16]. We do not address the well-posedness when $g^\varepsilon = g^\varepsilon(x, t)$, but show at least that (2.3.2) is equivalent to (2.3.1) with the same boundary data for classical solutions.

Let us therefore assume that there exists a differentiable function $s : K^c \to [0, \infty)$,

$Ds \neq 0$ for $t > 0$, such that $z \in C^2(Q_+) \cap C^1(\overline{Q_+}) \cap C^1(Q_-) \cap C(\overline{Q_-})$, $z > 0$ in Q_+, $z(x, s(x)) = 0$ if $s(x) > 0$, $z < 0$ in Q_- where

$$Q_\pm := \{(x,t) : x \in K^c,\ t > 0, \pm(t - s(x)) > 0\}.$$

By $z \in C(\overline{Q_-})$ we understand the z has a limit denoted as $z(x, s(x)-)$ as $(y,t) \to (x, s(x))$ along sequences with $t < s(y)$.

Assume that z satisfies (2.3.2), where the first equation is understood in the sense of distributions. Let us take a test function $\varphi \in C_c^\infty(K^c \times (0,\infty))$. We have

$$\begin{aligned} 0 &= \int_{K^c}\int_0^\infty cz\varphi_t + \beta(z)\Delta\varphi - \left(\frac{\partial}{\partial t}\frac{1}{g^\varepsilon}\right)\chi_{\text{int}\,\{z<0\}}\varphi \; dx\; dt = \\ &= \int_{Q^+} \beta(z)(c\varphi_t + \Delta\varphi)\; dx\; dt + \int_{Q^-} cz\varphi_t - \left(\frac{\partial}{\partial t}\frac{1}{g^\varepsilon}\right)\varphi \; dx\; dt := I_+ + I_-. \end{aligned}$$

Integration by parts on the individual terms $I_\pm$ yields

$$\begin{aligned} I_+ &= \int_{K^c}\int_{s(x)}^\infty c\beta(z)\varphi_t \; dt\; dx + \int_0^\infty \int_{\{s(x)<t\}} \beta(z)\Delta\varphi \; dx\; dt \\ &= -\int_{Q^+} (c\partial_t\beta(z) - \Delta\beta(z))\varphi \; dx\; dt - \int_0^\infty \int_{\{s(x)=t\}} D\beta(z)\cdot\frac{Ds}{|Ds|}\varphi \; d\mathcal{H}^{n-1}\; dt \end{aligned}$$

where we used that $z(x, s(x)) = 0$ and that the unit outer normal vector to $\{x : s(x) < t\}$ is $\frac{Ds}{|Ds|}$, and

$$I_- = \int_{Q_-} \left(-cz_t - \left(\frac{\partial}{\partial t}\frac{1}{g^\varepsilon}\right)\right)\varphi \; dx\; dt + \int_{K^c} cz(x, s(x)-)\varphi(x, s(x))\; dx.$$

From this we immediately have that $u = \beta(z)$ satisfies $cu_t - \Delta u = 0$ in Q_+, and $z = -\frac{1}{cg^\varepsilon}$ in Q_-. In particular, $z(x, s(x)-) = -\frac{1}{cg^\varepsilon(x,s(x))}$. The coarea formula yields

$$\int_0^\infty \int_{\{s(x)=t\}} D\beta(z)\cdot\frac{Ds}{|Ds|}\varphi \; d\mathcal{H}^{n-1}\; dt = \int_{K^c} D\beta(z)\cdot Ds\varphi(x, s(x))\; dx.$$

Therefore

$$\int_{K^c} \left(-\frac{c}{cg^{\varepsilon}(x, s(x))} - Du(x, s(x)) \cdot Ds(x) \right) \varphi(x, s(x)) \, dx = 0.$$

But $V = \frac{1}{|Ds|}$ and $-Du \cdot Ds = |Du||Ds|$ and therefore we conclude that

$$V = g^{\varepsilon}|Du|.$$

Chapter 3

Stefan Problem

3.1 Stefan Problem

On the other hand, Stefan problem appeals Hele-shaw equation as the zero heat limit of One-phase Stefan problem. Mathematically they have almost the same equation structure, except in the heat operator. One-phase of Stefan problem itself describes a melting of ice with a region of water, where the temperature of the ice is preserved to be zero. The retained interests are to obtain the temperature in the water area and to understand the phase interface between ice and water.

Surely solving Stefan problem numerically in enthalpy form is more straightforward than the temperature form. [17] implemented straightforward implicit finite difference to the enthalpy formulation of Stefan problem, and show the convergence of solution of the used modification Gauss-seidel method in order to solve a linear system.

In Stefan problem, refer to conservation law for energy, the change of heat amount per unit volume is $u = \rho c_P T$ where c_P is the specific heat at constant pressure and T is a temperature. The heat flux has two components due to conduction

and transport. The flux from conduction is $q = -k\nabla T$ where k denotes thermal conductivity. And the transport flux is $\rho c_P TV$ on the region of phase change. Therefore the heat equation can be described by the following equation with assuming ρ, c_P, and k are constant.

$$\begin{aligned} \frac{\partial T}{\partial t} &= \frac{k}{\rho c_P}\Delta T \text{ , in the water area} \\ \frac{\partial T}{\partial t} &= 0 \text{ , in the ice area} \\ \frac{\partial T}{\partial t} &= \nu_S \cdot \nabla T \text{ , on the phase change area.} \end{aligned} \tag{3.1.1}$$

Nevertheless, this work will consider the weaker form of (3.1.1) which physically describing the energy or more exactly enthalpy heat in the whole system. Given as the following equation for some parameter ϵ.

$$cu_t = \Delta h(u) \tag{3.1.2}$$

Where $h(u)$ is defined as

$$h(u) = u^+ \tag{3.1.3}$$

represents the temperature.

We are interested in developing an efficient numerical method to find a free boundary decently and more importantly to adjust the solution of averaging velocity in a periodic media.

The weak formulation for Stefan problem is based on the extension of the equation in term of temperature to the enthalpy energy balance, where the energy indicates the absence of jump at the critical temperature due to the change of phase.

3.1.1 Enthalpy Formulation

Since the free boundary position is unknown and has to be determined each time t, numerically the solution of (SF1) cannot be obtained straightforward. Technically in the numeric point of view, it is simpler to consider the problem in the form of enthalpy energy equation instead than directly solving the equation (SF1).

Let $u(\cdot,\cdot) : \mathbb{R}^n \times \{t > 0\} \to \mathbb{R}$. Physically $u(x,t)$ can be describe the enthalpy per unit volume at position x and t. The enthalpy energy in the system consists of the heat energy and the work to change the physical state of the material. The enthalpy energy in the solid and liquid region can be written as

$$u(x,t) = \begin{cases} \rho k_s(T(x,t) - T_{melting}) & ,T(x,t) < T_{melting} \text{ in solid region} \\ \rho k_l(T(x,t) - T_{melting}) + \rho L & ,T(x,t) > T_{melting} \text{ in the liquid region.} \end{cases} \tag{3.1.4}$$

where L is latent energy equals to $-1/g$ in problem (SF1), k_s and k_l are respectively specific heat of solid and liquid. In one-phase case, when the temperature in solid state is preserved to be equal to $T_{melting} = 0$, we define $\beta(\cdot) : \mathbb{R} \longmapsto [0,\infty)$ is mapping the enthalpy to the temperature in one-phase ice and water region, such that $\beta(u) = u^+$. We realize that there exist a jump at critical temperature $T_{melting}$ due to the change of phase caused by L, which in our case is not constant.

Thus, the enthalpy form of one-phase Stefan problem (with $\rho = 1$) is given by (SF2), where $c = k_l$.

$$\begin{cases} cu_t - \Delta\beta(u) = 0 & \text{in } (\mathbb{R}^n \setminus K) \times (0,\infty) \\ u = 1 & \text{in } K \times (0,\infty) \\ u(\cdot,0) = u_0 & \text{in } \mathbb{R}^n \end{cases} \tag{SF2}$$

3.1.2 Normal Velocity Derivation

Obviously since β is not even differentiable wherever $u = 0$, (SF2) can not give a point-wise interpretation to (SF1). Then, the equation can only be understood in the sense of distribution or weak sense. Formally we multiply (SF2) both side with test function $\varphi(x,t) \in C_c^\infty((\mathbb{R}^n \setminus K) \times (0,\infty))$ and do integration by part. Let denote $\mathbf{Q} := (\mathbb{R}^n \setminus K) \times (0,\infty)$, then we do the following computation.

$$
\begin{aligned}
&cu_t - \Delta\beta(u) = 0 \text{ in } \mathbf{Q} \\
&\qquad \Rightarrow \int_{\mathbf{Q}} (cu_t - \Delta\beta(u))\varphi dxdt = 0 \text{ for any test function } \varphi(x,t) \in C_c^\infty(\mathbf{Q}) \\
&\Rightarrow 0 = c\int_{\mathbf{Q}} u_t\varphi dxdt - \int_{\mathbf{Q}} \Delta\beta(u)\varphi dxdt \\
&\qquad = -c\int_{\mathbf{Q}} u\varphi_t dxdt + c\int_{\mathbb{R}^n\setminus K} u(x,0)\varphi(x,0)dx \\
&\qquad + \int_{\mathbf{Q}} \nabla\beta(u)\cdot\nabla\varphi dxdt - \int_{\partial(\mathbb{R}^n\setminus K)\times(0,\infty)} \nabla\beta(u)\cdot\nu\varphi dS(x)dt \\
&\qquad = \int_{\mathbf{Q}} \left(-cu\varphi_t + \nabla\beta(u)\cdot\nabla\varphi\right) dxdt \\
&\qquad = \int_{\mathbf{Q}} \left(-cu\varphi_t - \beta(u)\Delta\varphi\right) dxdt + \int_{\partial(\mathbb{R}^n\setminus K)\times(0,\infty)} \beta(u)\frac{\partial\varphi}{\partial\nu}dxdt \\
&\qquad \Rightarrow \mathbf{0} = \int_{\mathbf{Q}} \left(\mathbf{cu\varphi_t + (\beta u)\Delta\varphi}\right) \mathbf{dxdt}
\end{aligned}
\tag{3.1.5}
$$

Solution u of (3.1.5), is a weak solution (in distribution sense) of (SF2). And the equation (3.1.5) is called weak form of (SF2).

We denotes $\{u > 0\} := (\Omega_t \setminus K)\times(0,\infty)$ and $\{u < 0\} := \Omega_t^c \times (0,\infty)$. The area $\mathbf{Q}$ can be split satisfying $\mathbf{Q} := \overline{\{u > 0\}} \cup \{u < 0\}$, such that to be more specific we observe the weak form in the following cases. We assume that $u \in C(\overline{\{u > 0\} \cup \{u < 0\}})$, $\beta(\cdot) \in C^{2,1}(\overline{\{u > 0\}})$, and $\beta(\cdot) \in C^{2,1}(\overline{\{u < 0\}})$.

For $\varphi \in C_c^\infty(\{u>0)\}$

$$
\begin{aligned}
0 &= \int_{\mathbf{Q}} (cu\varphi_t + \beta(u)\Delta\varphi)\, dxdt \\
&= \int_{\{\mathbf{u>0}\}} (cu\varphi_t + \beta(u)\Delta\varphi)\, dxdt \\
&= \int_{\{\mathbf{u>0}\}} (-cu_t\varphi - \nabla\beta(u)\cdot\nabla\varphi)\, dxdt + \int_{\Omega_t\setminus K} cu(x,0)\varphi(x,0)dx \\
&+ \int_{\partial(\Omega_t\setminus K)\times(0,\infty)} \beta(u)\frac{\partial\varphi}{\partial\nu_x} dSdt, \text{ (integration by part)} \\
&= \int_{\{\mathbf{u>0}\}} (-cu_t\varphi - \nabla\beta(u)\cdot\nabla\varphi)\, dxdt + 0 \\
&= \int_{\{\mathbf{u>0}\}} (-cu_t\varphi + \Delta\beta(u)\varphi)\, dxdt - \int_{\partial(\Omega_t\setminus K)\times(0,\infty)} \nabla u\cdot\nu_x\varphi dSdt, \text{ (integration by part)} \\
&= \int_{\{\mathbf{u>0}\}} -(cu_t - \Delta u)\varphi dxdt + 0 \\
&\Rightarrow cu_t - \Delta u = 0
\end{aligned}
\tag{3.1.6}
$$

For $\varphi \in C_c^\infty(\{u<0\})$,

$$
\begin{aligned}
0 &= \int_{\{\mathbf{u<0}\}} (cu\varphi_t + \beta(u)\Delta\varphi)\, dxdt \\
&= \int_{\{\mathbf{u<0}\}} (cu\varphi_t)\, dxdt, \text{ (since } \beta(u)=0 \text{ in } \{u<0\}) \\
&= \int_{\{\mathbf{u<0}\}} (-cu_t\varphi)\, dxdt, \text{ by integration by part} \\
&\Rightarrow cu_t = 0
\end{aligned}
\tag{3.1.7}
$$

Moreover, it is necessary to observe a weak form through the interface. In purpose to obtain the formula for normal velocity on the interface, we assume the common boundary of $\{u>0\}$ and $\{u<0\}$ is a smooth surface in $\mathbb{R}^{n+1}$, and the complete unit outer normal vector of $\{u>0\}$ denoted by $\nu = (\nu_t, \nu_x)$. So therefore we do

this following computation

$$\begin{aligned}
0 &= \int_{\mathbf{Q}} (cu\varphi_t + \beta(u)\Delta\varphi)\, dxdt \\
&= \int_{\mathbf{Q}} -cu\varphi_t + \nabla\beta(u)\cdot\nabla\varphi dxdt \ , \forall\varphi \in C_c^\infty(\mathbf{Q}) \\
&= \int_{u>0} -cu\varphi_t + \nabla\beta(u)\cdot\nabla\varphi dxdt + \int_{u<0} -cu\varphi_t + \nabla\beta(u)\cdot\nabla\varphi dxdt \\
&= \int_{u>0} (cu_t - \Delta u)\varphi dxdt + \int_{\partial\{u>0\}} (-cu, \nabla u)\cdot(\nu_t, \nu_x)\varphi dS(x,t) \\
&+ \int_{u<0} cu_t\varphi - 0\varphi dxdt + \int_{\partial\{u<0\}} (-cu, 0)\cdot(-\nu_t, -\nu_x)\varphi dS(x,t) \\
&= \int_{\partial\{u>0\}} \left(-cu|^+\nu_t + \nabla u|^+\cdot\nu_x + cu|^-\nu_t\right)\varphi dS(x,t)
\end{aligned} \tag{3.1.8}$$

Therefore, on the free boundary of $\{u > 0\}$, it is satisfied the following formula.

$$\nabla u|^+\cdot\nu_x + cu|^-\nu_t = 0 \text{ on } \partial\{u>0\} \tag{3.1.9}$$

Normal vector on the moving boundary.

$$(\nu_t, \nu_x) = \frac{1}{\sqrt{(u_t|^+)^2 + |\nabla u|^+|^2}}(u_t|^+, \nabla u|^+)$$

Therefore, the formula for the normal velocity can be written as follow.

$$\begin{aligned}
0 &= \nabla u|^+\cdot\nu_x + cu|^-\nu_t \\
&= |\nabla u|^+|^2 + cu|^- u_t^+ \\
&\Rightarrow \frac{u_t^+}{|\nabla u|^+|} = \frac{-|\nabla u|^+|}{cu|^-} = \frac{1}{c}g(x)|\nabla u|
\end{aligned} \tag{3.1.10}$$

Considering u from the negative side as, $u|^- = -\frac{1}{g^c(x)} = -\frac{1}{cg(x)}$, we will obtain the same formula of normal velocity as in Hele-Shaw equation (HS). Therefore, by taking limit $c \to 0$ the solution of Latent heat problem (SF2) in area $\{u > 0\}$ is

expected to approach the given Hele-Shaw Problem, where $\{x \in \mathbb{R}^n | (x,t) \in \{u > 0\}\}$ was denoted as Ω_t in the Hele-Shaw equations.

It implies to the chosen of initial data u_0. Therefore if we expect to approximate HS by system (SF2), the initial data u_0 require to be the following form,

$$u_0 = \mathbf{1}_K + \mathbf{1}_{\Omega_0 \setminus K} v - \mathbf{1}_{\overline{\Omega_0}^c} \frac{1}{g^c} \tag{3.1.11}$$

where Ω_0 is a given initial domain, and v is harmonic function in $\Omega_0 \setminus K$.

Meanwhile, in one-phase Stefan problem such an ice melting, the problem is to find a function $T(x,t)$ and free boundary $\partial\Omega_t$ which satisfying:

$$\begin{cases} cT_t - \Delta T(x,t) = 0 & \text{for } (x,t) \in (\Omega_t \setminus K) \times (0,\infty) \\ T_t = g(x,t)|\nabla T|^2, & \text{for}(x,t) \in \partial\Omega_t \times (0,\infty) \\ T(x,t) = 1 & \text{for}(x,t) \in K \times (0,\infty) \\ T(x,t) = 0 & \text{for}(x,t) \in \overline{(\mathbb{R}^n \setminus \Omega_t)} \times (0,\infty) \\ T(x,0) = T_0(x) & \text{for } x \in \mathbb{R}^n \end{cases} \tag{SF1}$$

The problem models the ice material contacting the water, which in one-phase case the ice temperature is preserved to be $0°C$. The constant c represent a specific heat of water, and $-1/g(x,t)$ represents the latent energy of ice with $g > 0$.

In [18], it discusses the asymptotic convergence of the SF to HS. It states for 1 dimensional case when $g(x,t)$ is constant in x and t, the self-similar solution of u and T converge to the same constant as $t \to \infty$ for every fixed $x > 0$, Yet the convergence is not uniform. Despite the free boundary of both problem have the same growth rate $\sqrt{t}$, the free boundary of 1-D Stefan problem converge to Hele-Shaw when $c \to 0$.

Different to the 1-D case, problem SF is not ultimately to be HS as $t \to \infty$, for $n >= 2$ there is only the convergence behavior to a stationary state of both problem, and the asymptotic behavior is different. Meanwhile, in 2-dimensional case, it shows that the SF simplifies to HS. Unlikely in the 1-D case, the HS and SF problem for multidimensional spaces do not always have a classical solution. However, they always have a weak solution globally in time.

Chapter 4

Explicit Methods and Implementation

4.1 Explicit Finite Difference Method

4.1.1 Discretization Scheme for One Dimensional Case

In this section we explain how to apply explicit finite difference to obtain numeric solution for u of (SF2). In the scheme, we implement the explicit form, so that the computation is restricted by the stability condition. In order to apply Finite Difference Method for numerical purpose, space domain in problem (SF2) restricted to be bounded, such that for 1-D case we consider problem (4.1.1).

$$\begin{cases} cu_t - \Delta\beta(u) = 0 & \text{in } (0, X_{max}) \times (0, \infty) \\ u = 1 & \text{in } (-\infty, 0] \times (0, \infty) \\ \beta_x(u)(X_{max}, t) = 0 & \text{for } t \in (0, \infty) \\ u(x, 0) = \mathbf{1}_{(-\infty,0]} + \mathbf{1}_{(0,x_f(0))}v - \mathbf{1}_{[x_f(0),X_{max})}\frac{1}{g^c} & \end{cases} \tag{4.1.1}$$

where v is a linear decrease monotone function in $(1, x_f(0))$ with $v(0) = 1$.

4.1.1.1 Numerical Scheme

Let M be a number of discretization points for domain of x such that for some X_{max} satisfying $(0, x_f(t)) \subset [0, X_{max})$, $\Delta x = \frac{X_{max}}{M}$.
And u_i^k denote a value of solution u in the discrete note $(i\Delta x, k\Delta t)$. The discretized scheme for the equation $cu_t = \Delta\beta(u)$ can be written by standard Finite difference scheme as:

$$u_i^{k+1} = u_i^k + \left(\frac{\Delta t}{c\Delta x^2}\right)\left(\beta(u_{i-1}^k) - 2\beta(u_i^k) + \beta(u_{i+1}^k)\right) \tag{4.1.2}$$

for $k = 0, 1, \cdots, N_T$ and $i = 1, 2, \cdot, M-1$
with stability condition,

$$\frac{\Delta t}{c\Delta x^2} < \frac{1}{2}. \tag{4.1.3}$$

4.1.1.2 Adjusting Free Boundary Position

In solving Hele-Shaw problem through the Stefan equation describe above, It is noteworthy to decently adjust the free boundary position in the problem. For one-dimension case we consider that numeric position of free boundary is computed as :

$$x_f^k = \min\{x_i | u_i^k u_{i+1}^k < 0, i = 0, 1, ..., M-1\} \tag{4.1.4}$$

or by interpolation as described at figure 4.1, such that the free boundary position is approximated as formula (4.1.5).

$$x_f^k \approx \hat{x_f} = x_i + \Delta x\left(\frac{u_{i-1}^k}{u_{i-1}^k - u_i^k} - 1\right) \tag{4.1.5}$$

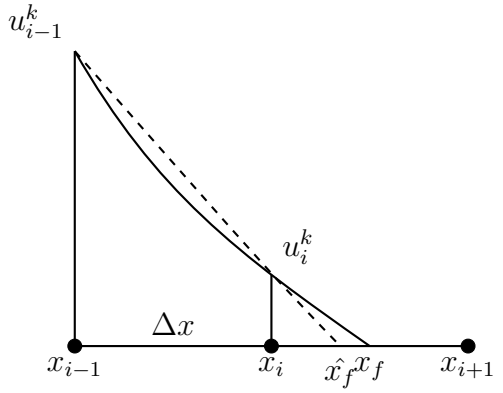

FIGURE 4.1: Extrapolation to estimate $\bar{x_f}$

4.1.2 The scheme for Two Dimensional Case

Let $D \subset \mathbb{R}^2$ be a bounded rectangle domain, and given closed set $K \subset D$. In order to apply finite difference method in 2-D case, we assume u always be differentiable on ∂D such that for numerical purpose, we consider problem (4.1.6),

$$\begin{cases} cu_t - \Delta\beta(u) = 0 & \text{in } (D \setminus K) \times (0, \infty) \\ u(\cdot, t) = 1 & \text{in } K \times (0, \infty) \\ \frac{\partial\beta(u)}{\partial n} = 0 & \text{on } \partial D \times (0, \infty) \\ u(\cdot, 0) = u_0 & \text{in } \mathbb{R}^n \end{cases} \tag{4.1.6}$$

where the initial condition u_0 follows the form at (3.1.11).

4.1.2.1 Numerical Scheme

We assume that $\Delta y = \Delta x$. The discretization scheme of explicit method for (4.1.6) as follows.

$$\begin{aligned} u_{i,j}^{k+1} = & \\ & u_{i,j}^k + \left(\frac{\Delta t}{c\Delta x^2}\right) \{\beta(u_{i-1,j}^k) \\ & + \beta(u_{i+1,j}^k) - 4\beta(u_{i,j}^k) + \beta(u_{i,j+1}^k) + \beta(u_{i,j-1}^k)\} \end{aligned} \tag{4.1.7}$$

with stability condition,

$$\frac{\Delta t}{c\Delta x^2} < \frac{1}{4}. \tag{4.1.8}$$

4.1.2.2 Adjusting Numeric Free Boundary in 2D Cartesian Grid

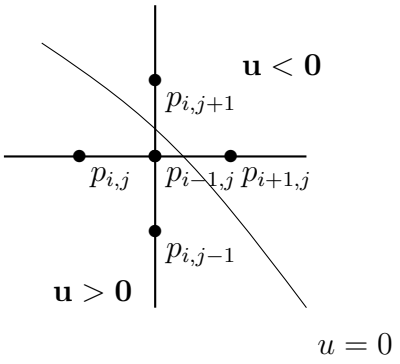

FIGURE 4.2: Boundary lies on the Cartesian grid between a 5-point stencil

Similarly to the scheme explained above. In order to adjust free boundary position lying on the Cartesian grid, we consider the situation of boundary across the grid between the 5-point stencil, where the center point as the reference. Figure 4.2 describes a situation when the boundary lies on the grid in 5-point stencil, where $p_{i,0}$ is a reference point. Since in our case, the boundary represents $\partial\{u > 0\}$ where the solution of Hele-shaw defined, we consider $P_{i,0}$ which returning $u > 0$ as the approximation of boundary position.

We may also extrapolate the position of free boundary crossing the legs of a 5-point stencil, by using two closest points in $\{u > 0\}$ side straight through the edge.

4.2 Numerical Results and Discussion

4.2.1 One Dimensional Case

Let $K = (-\infty, 0]$, $\Omega_0 = (-\infty, x_f(0))$ for given $x_f(0)$, and $K \subset \Omega_0$, and $\Omega_t = (-\infty, x_f(t))$. The exact solution of 1-dimensional Hele-Shaw problem for the given

Ω_0 and K is as follow.

$$u(x,t) = \begin{cases} 1 & \text{, for } (x,t) \in K \times [0,\infty) \\ 1 - \frac{x}{x_f(t)} & \text{, for } (x,t) \in \Omega_t \setminus K \times [0,\infty), x_f(t) > 0 \\ 0 & \text{, for } (x,t) \in \overline{\Omega_t}^c \times [0,\infty) \end{cases} \tag{4.2.1}$$

and the velocity at $x_f(t)$ is given by:

$$V_n = x_f'(t) = g(x_f,t)|\nabla u(x_f,t)| = \frac{g(x_f,t)}{x_f(t)}, \text{ by taking constant } g(x,t) = 1 \tag{4.2.2}$$

and noticing that $x_f(t)$ is non-decreasing function with $x_f(0) > 0$, we obtain :

$$\frac{dx_f(t)}{dt} = \frac{1}{x_f(t)}$$

$\Rightarrow x_f(t) = \sqrt{2t + x_f(0)}$ is the solution of free boundary for this particular case.

4.2.1.1 Numerical Solution

To confirm the accuracy, we implement the scheme to the particular case and compare the result to its analytic solution.

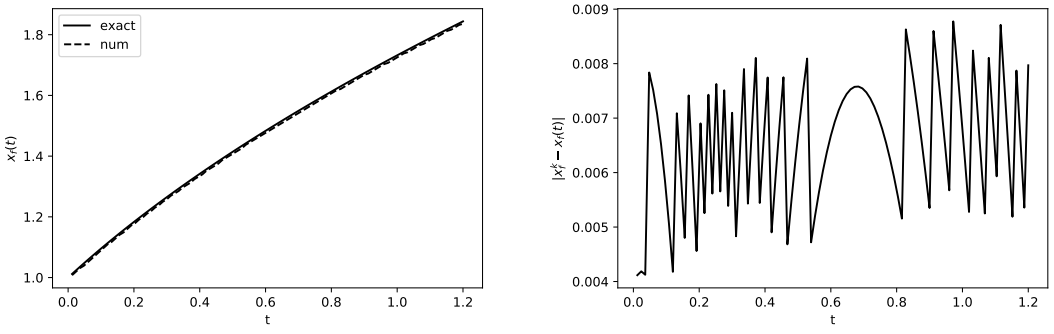

FIGURE 4.3: Free Boundary Position and its absolute error

Figure 4.3 shows the numerical solution of free boundary position in time from Finite Difference Method (showing on the left), and its error computation, $e =$

$|x_f^k - x_f(k\Delta t)|$ (on the right). We can see from the error that the method is not satisfying enough, $\max_t |e| > \Delta x$ for small enough $\epsilon = 10^{-4}$. Figure 4.4 shows the error of numerical solution is still big enough. Nevertheless, it shows an error reduction in time.

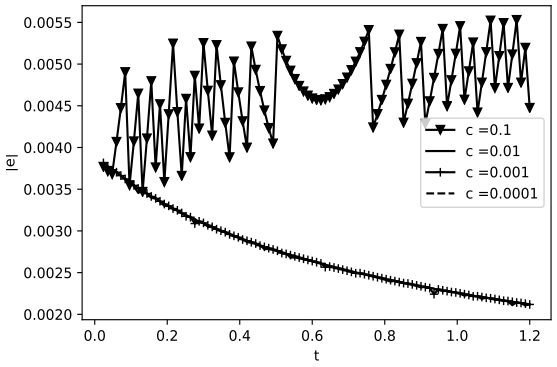

FIGURE 4.4: Maximum error of Solution in time, with $\Delta x = 0.004$ and $\epsilon = 0.0001$

4.2.1.2 Numerical Error of Solution and Free Boundary Position

We observe the truncation error of the finite difference method and the error caused by parameter heat specific parameter c. Figure 4.5 shows the error behavior either for the numerical solution of HS problem and the free boundary position influenced by c and Δx. Figure 4.5 shows the maximum error of numerical solution during computation per time step affected by Δx and c, $e = \max_{x,t} |u_{Num} - u|$. We conclude that for the small c, Finite Difference scheme (4.1.2) gives only the error order 1. In the figure 4.6 we can observe the error of free boundary position during computation per time step affected by Δx and c, $e = \max_{x,t} |x_{fNum} - x_f|$. We conclude that for the small c, the scheme gives only the error order up to 1. The smaller c after some level does not give significant error reducing in both solutions, which is what we expecting.

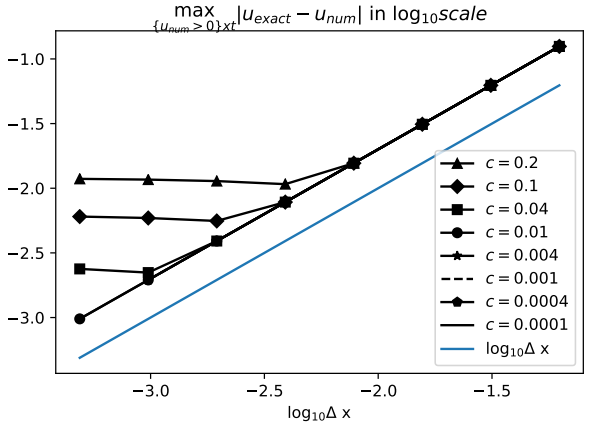

FIGURE 4.5: Error of numerical solution in the logarithmic scale.

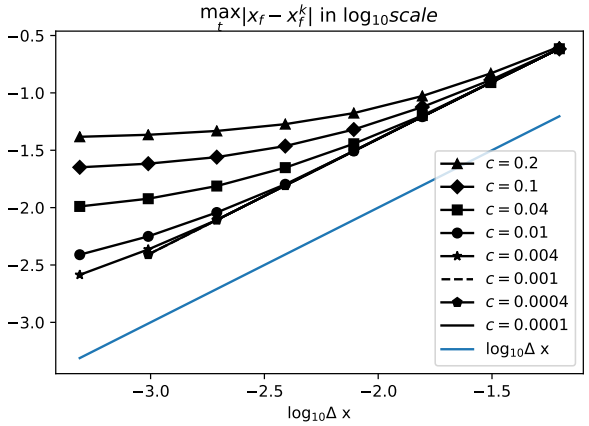

FIGURE 4.6: Error of numeric free Boundary Position in the logarithmic scale.

4.2.2 Two Dimensional case

Suppose that $K = \overline{B(0, R_k)} \subset \mathbb{R}^2$, $\Omega_0 = B(0, R_f(0)) \subset \mathbb{R}^2$, $R_f(0) = R_0$, and $K \subset \Omega_0$, and $\Omega_t = B(0, R_f(t))$ denotes a domain at time t.The exact solution of Hele-Shaw equation as (HS) for the given Ω_0 and K is as follows.

$$u(x,t) = \begin{cases} 1 & , \text{for } x \in K \\ \frac{\log|x| - \log R_f(t)}{\log R_k - \log R_f(t)} & , \text{for } x \in \Omega_t \setminus K \\ 0 & , \text{for } x \in \overline{\Omega_t}^c \end{cases} \tag{4.2.3}$$

with a normal velocity is given by :

$$V_n(x) = g(x,t)|\nabla u(x,t)| \text{ , for } x \in \partial(\Omega_t \setminus K) \tag{4.2.4}$$

For particular case, by taking $g(x) = 1$ we have radially symmetry behavior for the position of free boundary against the center point. Therefore, for $R_f(t) = |x|, x \in \partial(\Omega_t \setminus K) \subset \mathbb{R}^2$ we can write:

$$V_n = R_f'(t) = g(x)|\nabla u(x)| = \frac{g(x)}{\log|\frac{R_k}{|x|}||x|} = \frac{1}{R_f(t)\log\frac{R_k}{R_f(t)}} \tag{4.2.5}$$

We expect to obtain explicitly the formula for $R_f(t)$, which appears as the ordinary differential equation. Yet for the numerical purpose, it is sufficient to compute the exact solution by fourth-order Runge-Kutta approximation method.

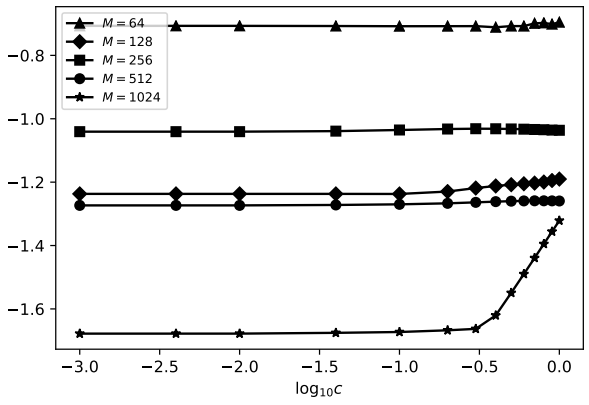

FIGURE 4.7: Maximum absolute error of solution with x-axis ϵ

4.2.2.1 Numerical Solution in Periodic Media

We experiment for one example $g(x)$ with $c = 4$ in Figure 4.9. We expect faster and better computation rather than using explicit finite different. We also observe from the Figure 4.10, 4.11, and 4.12, there must be reasonable set between mesh

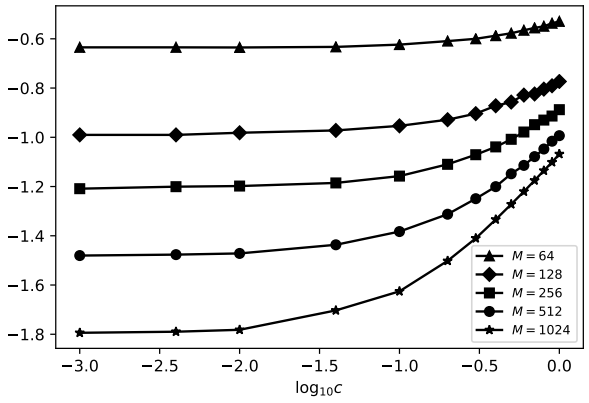

FIGURE 4.8: Maximum absolute error of free boundary with x-axis ϵ

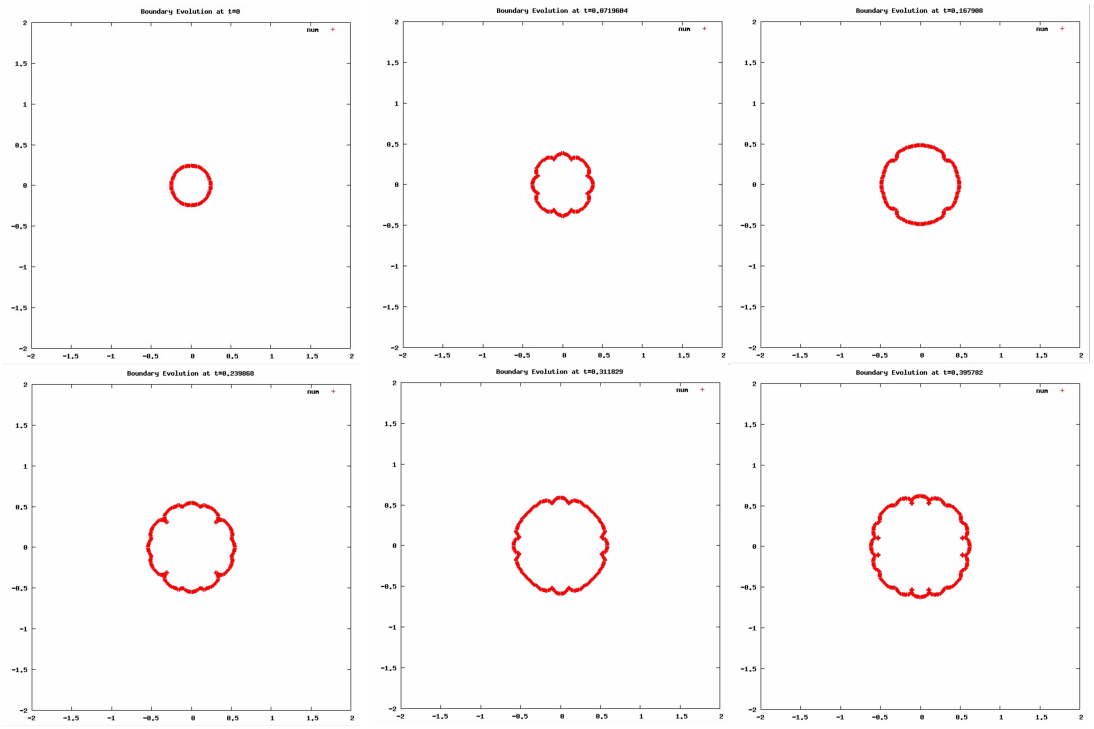

FIGURE 4.9: Maximum absolute error of solution with x-axis ϵ

size M and the oscillating coefficient ϵ. We can see ffrom the pictures, on the mesh size with $M = 128, 256$ the error obtained from $\epsilon = 0.1$ is smaller than the $\epsilon = 0.01$ has, but the value is closer to the $\epsilon = 0.001$.

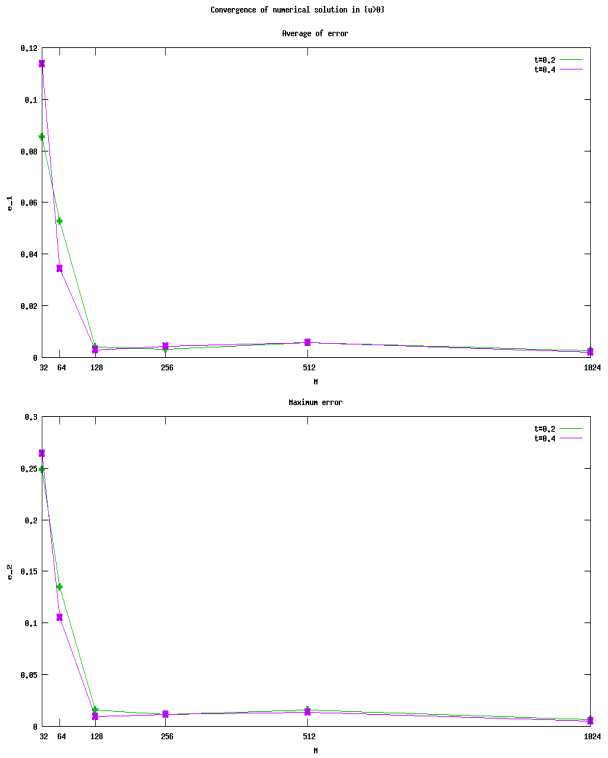

FIGURE 4.10: Error behavior for $g(x,t) = \sin(\frac{2x-t}{0.1})$

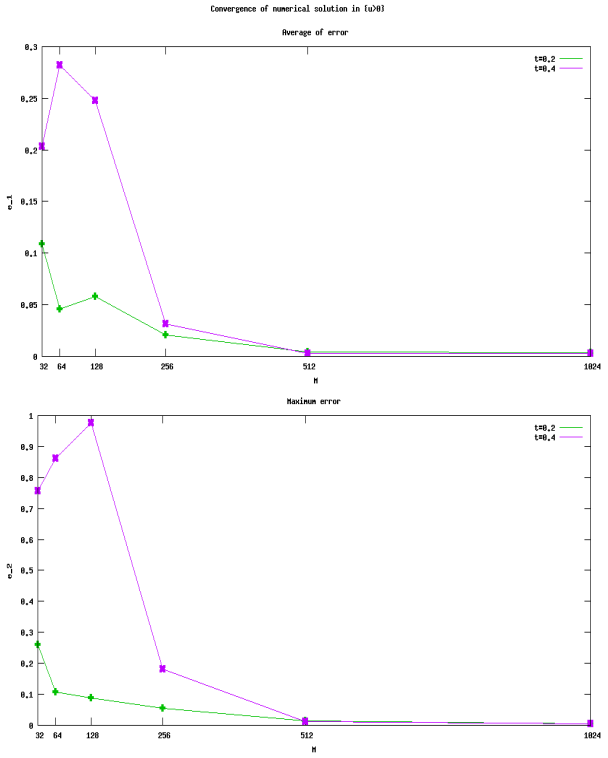

FIGURE 4.11: Error behavior for $g(x,t) = \sin(\frac{2x-t}{0.01})$

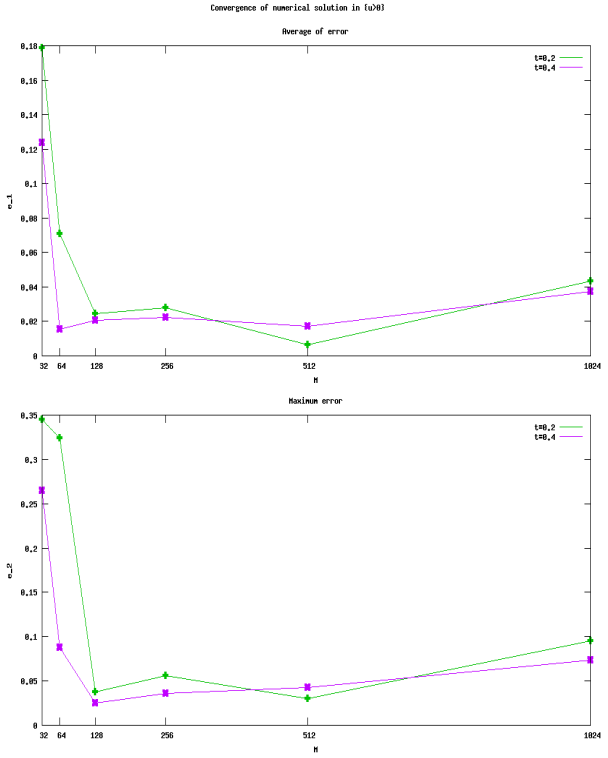

FIGURE 4.12: Error behavior for $g(x,t) = \sin(\frac{2x-t}{0.001})$

Chapter 5

BBR Scheme as an Efficient Method

A numerical solution of problem (2.3.2) can be found efficiently by the method introduced by Berger, Brézis and Rogers [5], in the form further studied by Murakawa [19]. We refer to this scheme as the BBR scheme. Choosing a time step $\tau > 0$, we iteratively find the sequences $\{u^k\}_{k\geq 1}$, $\{z^k\}_{k\geq 0}$ of solutions of

$$\begin{cases} c\mu^{k-1}u^k - \tau\Delta u^k = c\mu^{k-1}\beta(z^{k-1}) & \text{in } U, \\ \dfrac{\partial u^k}{\partial x_1}(0,\cdot) = q_1, \\ u^k(1,\cdot) = 0, \\ u^k \qquad \text{1-periodic in } x_2, \end{cases} \tag{5.0.1a}$$

$$z^k = z^{k-1} + \mu^{k-1}(u - \beta(z^{k-1})) - \frac{\tau}{c}\left(\frac{\partial}{\partial t}\frac{1}{g^\varepsilon}\right)(\cdot, t_{k-\frac{1}{2}})\chi_{\text{int}\{z^{k-1}<0\}}, \tag{5.0.1b}$$

$$\mu^k = \frac{1}{\delta + \beta'(z^k)}, \tag{5.0.1c}$$

for $k = 1, 2, \ldots$, with $z^0 := z(\cdot, 0)$. Here $\delta > 0$ is a chosen regularization parameter that we discuss below, and we define

$$\beta'(s) := \begin{cases} 1, & s > 0, \\ 0, & s \leq 0. \end{cases}$$

Note that we add the source $-\frac{1}{c}\left(\frac{\partial}{\partial t}\frac{1}{g^\varepsilon}\right)(\cdot, t_{k-\frac{1}{2}})\chi_{\text{int}\{z^{k-1}<0\}}$, $t_{k-\frac{1}{2}} = (k-\frac{1}{2})\tau$, to the update of z in (5.0.1b) rather than the problem (5.0.1a) as was done in [5]. This is to avoid any unwanted diffusion in $\{z < 0\}$ that would otherwise occur.

Let us comment on the choice of τ, δ and c. The time step restriction comes from the fact that the free boundary can advance at most distance h (one node distance) in one-time step. We therefore take the time step $\tau < \frac{h}{2V_{\max}}$, where $V_{\max}$ is some reasonable estimate on the maximum velocity of the free boundary in the problem.

The maximum principle yields $u^k > 0$ on U. The regularization parameter $\delta > 0$ guarantees a presence of a boundary layer in the neighborhood of the free boundary where u^k is sufficiently large so that z is increasing there. Let us estimate its width. Assuming a one-dimensional situation for simplicity, with free boundary position of z^{k-1} located at $x_1 = 0$ with $z^{k-1} < 0$ for $x_1 > 0$, (5.0.1a) simplifies in $\{x_1 > 0\}$ to

$$\frac{c}{\delta}u^k - \tau u^k_{x_1 x_1} = 0,$$

and therefore the dominating term in the solution will be $\phi(x_1) = Ce^{-\sqrt{\frac{c}{\delta\tau}}x_1}$, where $C \approx -q_1\sqrt{\frac{\delta\tau}{c}}$ so that the derivative ϕ_{x_1} is approximately q_1 at $x_1 = 0$.

From (5.0.1b), the total amount of energy deposited into the negative z per one time step is therefore $\int_0^\infty z^k - z^{k-1}\, dx_1 = \frac{1}{\delta}\int_0^\infty \phi\, dx_1 \approx -q_1\frac{\tau}{c}$, which is as expected from Fourier's law. We need to choose $\delta > 0$ so that the majority is deposited near the free boundary $\{x_1 = 0\}$. The ratio deposited in $\{a < x_1\}$ for some $a > 0$ is given by $\int_a^\infty \phi\, dx_1 / \int_0^\infty \phi\, dx_1 = e^{-\sqrt{\frac{c}{\delta\tau}}a}$. For this to be equal to a given $\gamma \in (0, 1)$

with $a = wh$, $w > 0$, we need to take

$$\delta = \left(\frac{w}{\log \gamma}\right)^2 \frac{ch^2}{\tau}.$$

We have not observed any ill effect if we choose small w, so we in general set $w = 1$, $\gamma = 0.01$, which yields the formula

$$\delta \approx 4.7 \times 10^{-2} \frac{ch^2}{\tau}. \tag{5.0.2}$$

Let us explain how we implement the update of z in the set $\{z < 0\}$ in the BBR method (5.0.1b). Since the set $\{z > 0\}$ is monotonically increasing if z is the exact solution of (2.3.2), $z = -\frac{1}{cg^\varepsilon}$ in $\{z < 0\}$. However, in the BBR method (5.0.1b), the value of z^k is also influenced in $\left\{z^{k-1} < 0\right\}$ by u^k since $u^k > 0$ in U by the comparison principle. On the other hand, u^k decreases exponentially with the distance from $\left\{z^{k-1} > 0\right\}$ as observed above. We therefore make use of this fact and at a given fixed point x, we set $z^k(x) = -\frac{1}{cg^\varepsilon(x,t_k)}$ at the first time step k such that $u^k(x) > 10^{-3}\delta$, where δ is the regularization parameter in (5.0.1c), and only at the later time steps we apply the update (5.0.1b) at this node. This leads to a significant increase in the accuracy of the estimate of $r(q)$, especially in a neighborhood of the pinning intervals.

Since we need to find the solutions of the Hele-Shaw problem for many different q over a large time interval (relative to ε) to get a reliable estimate on $r(q)$, it is important to develop an efficient numerical method to solve the elliptic problem (5.0.1a) for u^k. It turns out that a multigrid scheme for the linear elliptic problem for u^k works well even though μ^{k-1} has a jump across the free boundary.

Chapter 6

Multigrid Method

6.1 Multigrid

In this section we focus on the linear elliptic problem

$$\begin{cases} au - h^2\Delta u = f & \text{in } U = (0,1)^2 \\ u_{x_1}(0, x_2) = q_1 & \text{for } x_2 \in [0,1) \\ u(1, x_2) = 0 & \text{for } x_2 \in [0,1) \\ u \quad \text{1-periodic in } x_2, \end{cases} \tag{6.1.1}$$

where $h > 0$ will be the discretization step and a is a given bounded nonnegative function.

We will choose $M = 2^p$ for some $p \in \mathbb{N}$ as the resolution and set $h = \frac{1}{M}$ and introduce $x_i = ih$, $i = 0, \ldots, M$. We discretize the PDE using the standard finite difference method with the central difference on a 5-point stencil. We therefore look for $v_{i,j}$, $i, j = 0, \ldots, M-1$, that approximate $u(x_i, x_j)$. For the Neumann boundary condition, we use a ghost grid point assuming $v_{-1,j} = v_{1,j} - 2q_1 h$. This

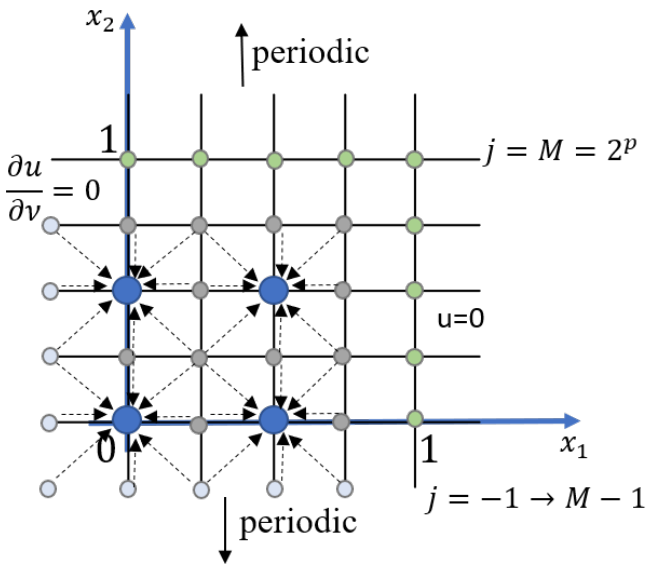

FIGURE 6.1: Transfer between grids, restriction and prolongation.

leads to the linear system

$$\begin{cases} (4 + a_{i,j})v_{i,j} - v_{i-1,j} - v_{i+1,j} - v_{i,j-1} - v_{i,j+1} = f_{i,j}, \\ \qquad\qquad i = 1, \ldots, M-1, j = 0, \ldots, M-1, \\ (4 + a_{i,j})v_{0,j} - 2v_{1,j} - v_{0,j-1} - v_{0,j+1} = f_{0,j} - 2q_1 h, \\ \qquad\qquad j = 0, \ldots, M-1, \\ v_{i,-1} = v_{i,M-1}, \\ v_{i,M} = v_{i,0}, \\ v_{M,j} = 0, \end{cases} \tag{6.1.2}$$

where $f_{i,j} := f(x_i, x_j)$ and $a_{i,j} := a(x_i, x_j)$.

To solve this system, we use the standard multigrid method, see for example [20]. We introduce a sequence of spaces

$$V^{2^m h} = \mathbb{R}^{(M/2^m - 1)\times(M/2^m - 1)}, \qquad m = 0, \ldots, p.$$

On each of these we will solve the linear system with appropriately adjusted M. We need to introduce the grid transfers. The restriction operator $I_h^{2h} : V^h \to V^{2h}$ is defined by the standard weighted sum

$$(I_h^{2h} v^h)_{i,j} = \frac{v^h_{2i,2j}}{4} + \frac{v^h_{2i-1,2j} + v^h_{2i+1,2j} + v^h_{2i,2j-1} + v^h_{2i,2j+1}}{8} + \frac{v^h_{2i-1,2j-1} + v^h_{2i+1,2j-1} + v^h_{2i-1,2j+1} + v^h_{2i+1,2j+1}}{16},$$

where we assume the periodic extension in j and we assume that v^h is even across $i = 0$, that is,

$$v^h_{-1,j} = v^h_{1,j},$$
$$v^h_{i,-1} = v^h_{i,M-1}, \qquad v^h_{i,M} = v^h_{i,0}.$$

This is motivated by the fact that the error correction will satisfy the boundary condition $u_{x_1}(0, x_2) = 0$.

The prolongation operator $I_{2h}^h : V^{2h} \to V^h$ is the standard prolongation

$$\begin{aligned}
(I_{2h}^h v^{2h})_{2i,2j} &= v^{2h}_{i,j}, \\
(I_{2h}^h v^{2h})_{2i+1,2j} &= \frac{1}{2}\left(v^{2h}_{i,j} + v^{2h}_{i+1,j}\right), \\
(I_{2h}^h v^{2h})_{2i,2j+1} &= \frac{1}{2}\left(v^{2h}_{i,j} + v^{2h}_{i,j+1}\right), \\
(I_{2h}^h v^{2h})_{2i+1,2j+1} &= \frac{1}{4}\left(v^{2h}_{i,j} + v^{2h}_{i,j+1} + v^{2h}_{i+1,j} + v^{2h}_{i+1,j+1}\right),
\end{aligned}$$

again assuming the periodic extension $v^{2h}_{i,M} = v^{2h}_{i,0}$.

By $A^{2^m h}$ we will denote the matrix of the linear system (6.1.2) for grid with resolution $M/2^m$ with $a^{2^m h}$ defined recursively as

$$a^{2h} = 4 I_h^{2h} a^h.$$

We perform the following multigrid V-cycle:

(a) k_1 times iterate the smoother for $A^h v^h = b^h$ with initial guess $v^{h,(0)}$, obtaining $v^{h,(k_1)}$.

(b) Find the residual $r^h = b^h - A^h v^{h,(k_1)}$

(c) Restrict the right-hand side $b^{2h} = 4I_h^{2h} r^h$.

(d) Solve $A^{2h} e^{2h} = b^{2h}$ on a half-resolution grid recursively.

(e) Correct the approximation $\tilde{v}^{h,(k_1)} = v^{h,(k_1)} + I_{2h}^h e^{2h}$.

(f) k_2 times iterate the smoother for $A^h v^h = b^h$ with initial guess $\tilde{v}^{h,(k_1)}$.

The problem $A^1 e^1 = b^1$ is solved exactly.

To improve the convergence, we solve for e^{2h} using two V-cycles, with initial guess $e^{2h} = 0$.

As a smoother we implement the damped Jacobi method with damping constant $\omega = \frac{2}{3}$. We perform $k_1 = k_2 = 4$ relaxation iterations. This reduces the maximum norm of the residual by about a factor of 10 per iteration, see Table 6.1.

To estimate the time complexity, we observe that the matrix multiplication and the application of prolongation and restriction operators have each approximately the time complexity of a single Jacobi iteration. With these parameters, a simple estimate places the time complexity of the V-cycle at about 22 Jacobi iterations. Moreover, the method is parallelizable in a straightforward manner. We did not explore this point since we need to run a large number of computations and therefore can take advantage of process-level parallelism.

iteration k	$\left\|r^{(k)}\right\|$
0	1.95×10^{-3}
1	3.11×10^{-5}
2	1.54×10^{-6}
3	8.95×10^{-8}
4	5.53×10^{-9}
5	3.43×10^{-10}
6	2.13×10^{-11}
7	1.33×10^{-12}
8	8.44×10^{-14}
9	5.88×10^{-15}
10	9.44×10^{-16}
11	7.77×10^{-16}

TABLE 6.1: Evolution of the residual in the multigrid method with $M = 1024$, $h = 1/M$, $b^h = 0$, $a_{i,j} = 1000h^2$ if $x_i + 0.1\sin(6\pi x_j) > 0.5$ and $a_{i,j} = h^2$ otherwise, and $f_{i,j} = 0$, with initial guess $v^h = 0$.

Chapter 7

Numerical Implementation for Hele-shaw Problem

7.1 Application of the multigrid solver to the BBR scheme

To find u^k in (5.0.1a), we apply the above multigrid solver to (6.1.1) with $a = \frac{ch^2}{\tau}\mu^{k-1}$ and $f = \frac{ch^2}{\tau}\mu^{k-1}\beta(z^{k-1})$, and we use u^{k-1} as the initial guess. In our computations it is generally sufficient to perform a fixed number of V-cycles per time step. We perform in general 1–3 V-cycles.

7.2 Estimating Error caused by non-periodic g

Now we estimate the error caused by approximating $\tilde{g}$ by a periodic function. Let $\omega = \frac{1}{\epsilon}$ be a number of oscillation and $n = \lfloor \omega \rfloor$ be a largest integer smaller that ω, such that $\tilde{g}$ is 1-periodic function in $[0, \epsilon n]^2 \subset [0, 1]^2$. If we write the average of

function $\langle\frac{1}{\tilde{g}}\rangle$ in unit rectangle $[0,1]^2$ as follow,

$$\begin{aligned}\langle\frac{1}{\tilde{g}}\rangle := \int_{[0,1]^2}\frac{1}{\tilde{g}(\frac{x}{\epsilon},\frac{y}{\epsilon})}dxdy &= \int_{[0,\epsilon n]^2}\frac{1}{\tilde{g}(\frac{x}{\epsilon},\frac{t}{\epsilon})}dxdt + \int_{[0,1]^2\setminus[0,\epsilon n]}\frac{1}{\tilde{g}(\frac{x}{\epsilon},\frac{y}{\epsilon})}dxdy \\ &= \epsilon n\langle\frac{1}{g}\rangle + \int_{[0,1]^2\setminus[0,\epsilon n]}\frac{1}{\tilde{g}(\frac{x}{\epsilon},\frac{y}{\epsilon})}dxdy\end{aligned}$$

then we can estimate,

$$\begin{aligned}\left|\langle\frac{1}{g}\rangle - \langle\frac{1}{\tilde{g}}\rangle\right| &\le \left|(1-(\epsilon n)^2)\langle\frac{1}{g}\rangle\right| + \left|\int_{[0,1]^2\setminus[0,\epsilon n]}\frac{1}{\tilde{g}(\frac{x}{\epsilon},\frac{y}{\epsilon})}dxdy\right| \\ &\le (1-(\epsilon n)^2\left[\left\langle\frac{1}{g}\right\rangle + \frac{1}{g_{min}}\right] \\ &= (1-(\frac{\lfloor\omega\rfloor}{\omega})^2)\left[\left\langle\frac{1}{g}\right\rangle + \frac{1}{g_{min}}\right] \\ &\le \frac{2}{\omega}\left[\left\langle\frac{1}{g}\right\rangle + \frac{1}{g_{min}}\right]\end{aligned}$$

such that the error of $r(q)$ caused by approximating function $\tilde{g}$ is bounded, depends on ω as the following computation.

$$\begin{aligned}\left|r(q) - \tilde{(}r)(q)\right| &= |q|\left|\frac{1}{\left\langle\frac{1}{g}\right\rangle} - \frac{1}{\left\langle\frac{1}{\tilde{g}}\right\rangle}\right| \\ &= |q|\left|\frac{\left\langle\frac{1}{\tilde{g}}\right\rangle - \left\langle\frac{1}{g}\right\rangle}{\left\langle\frac{1}{g}\right\rangle\left\langle\frac{1}{\tilde{g}}\right\rangle}\right| \\ &\le |q|\frac{2g_{max}}{\omega\left\langle\frac{1}{g}\right\rangle}\left[\left\langle\frac{1}{g}\right\rangle + \frac{1}{g_{min}}\right] \le C\frac{|q|}{\omega}\end{aligned}$$

Therefore, the error caused by approximating $\tilde{g}$ by periodic function goes smaller as ω increases.

7.3 General direction

So far we have assumed that $q = (q_1, 0)$ with $q_1 < 0$. To handle general $q \in \mathbb{R}^2 \setminus \{0\}$, we rotate the coordinate system so that q is of this form. That is, instead of g we consider

$$\tilde{g}(x,t) = g(x_1\nu + x_2\nu^\perp, t),$$

where $\nu^\perp = (-\nu_2, \nu_1) = \left(\frac{q_2}{|q|}, -\frac{q_1}{|q|}\right)$.

Of course, in general $\tilde{g}$ is not periodic in x_2, unless there exist integers $n_1, n_2 \in \mathbb{Z}$, $n_1 n_2 \neq 0$, such that $n_1 q_1 + n_2 q_2 = 0$, that is, unless q is a *rational* direction. These are however the only directions that we can consider numerically.

By taking $\sigma = \frac{q_1}{n_2} = -\frac{q_2}{n_1}$ and $m_1 = n_2$, $m_2 = -n_1$, it can be easily seen that q is a rational direction if and only if there exist $\sigma > 0$ and two integers $m_1, m_2 \in \mathbb{Z}$ such that $q = (m_1\sigma, m_2\sigma)$. Let us show how we can choose ε so that the solution of the ε-problem is 1-periodic in the x_2 direction. To this end, we shall find the minimal period of $\tilde{g}$ first. This is equivalent to finding the smallest $s > 0$ such that $s\nu^\perp \in \mathbb{Z}^2$.

Lemma 7.3.1. *If m_1 and m_2 are co-prime, then $s = (m_1^2 + m_2^2)^{\frac{1}{2}}$ is the smallest $s > 0$ such that $s\nu^\perp \in \mathbb{Z}^2$.*

Proof. Note that $\nu^\perp = \frac{(m_2, -m_1)}{(m_1^2+m_2^2)^{\frac{1}{2}}}$. Clearly

$$s\nu^\perp = (m_2, -m_1) \in \mathbb{Z}^2.$$

Now suppose that there is $0 < \tilde{s} < s$ such that $\tilde{s}\nu^\perp \in \mathbb{Z}^2$. But then $\frac{\tilde{s}}{s} s\nu^\perp = \frac{\tilde{s}}{s}(m_2, -m_1) \in \mathbb{Z}^2$. In particular $\frac{\tilde{s}}{s} \in \mathbb{Q}$. Suppose that $\frac{\tilde{s}}{s} = \frac{p}{q}$, where p, q are coprime.

Since $\frac{p}{q} < 1$, $q > 1$ is a divisor of both m_1 and m_2. But that is a contradiction with m_1 and m_2 being coprime. □

Given a general $q = (m_1\sigma, m_2\sigma)$, it is therefore sufficient to choose

$$\varepsilon = \frac{\gcd(m_1, m_2)}{d(m_1 + m_2)^{\frac{1}{2}}}$$

for some integer $d \in \mathbb{N}$ and the solution will be 1-periodic in the x_2 direction. Note that this limits the angular resolution of our method. For example, near the x_1-axis, to compute $q = (m_1\sigma, \sigma)$ near a fixed $\hat{q} = (\hat{q}_1, 0)$, we must take $\varepsilon < \frac{1}{m_1}$ which requires large resolution M for small σ since $m_1 = \frac{\hat{q}_1}{\sigma}$.

7.4 Numerical results

To test the numerical method, we estimate the homogenized velocity $r(q)$ for a few simple functions g. Namely, we consider

$$g(x,t) = \sin(2\pi(x_1 + t)) + 2, \tag{7.4.1a}$$

$$g(x,t) = \sin(2\pi(x_1 + t)) + \sin(2\pi(x_2 + t)) + 3, \tag{7.4.1b}$$

$$g(x,t) = \frac{1}{2}\cos(2\pi t)\Big(\sin(2\pi x_1) + \sin(2\pi x_2)\Big) + 2, \tag{7.4.1c}$$

$$g(x,t) = \sin(2\pi(x_1 + t)) + \sin(2\pi(x_1 + 3t)) + 3. \tag{7.4.1d}$$

By Lemma 2.2.1, the pinning interval with $r(q) = 1$ in (7.4.1a) is $[\frac{1}{3}, 1] \times \{0\}$. Note that (7.4.1c) is a superposition of four traveling waves moving with speed 1 in directions $(1,0)$, $(-1,0)$, $(0,1)$ and $(0,-1)$.

We always take $c = 10^{-7}$, $\tau = \frac{h}{8}$ and δ as in (5.0.2), and $L_0 = 0.1$, $L_1 = 0.9$. The values of $r(q)$ are estimated for a range of $q = (m_1\sigma, m_2\sigma)$, with $\sigma = \frac{6.4}{M}$,

$m_1, m_2 \in \mathbb{Z}$. For given q, we determine ε following Section 7.3 as

$$\varepsilon = \frac{1}{N(m_1^2 + m_2^2)^{\frac{1}{2}}}, \qquad N = \max\left(1, \operatorname{round}\left(\frac{9M}{64(m_1^2 + m_2^2)^{\frac{1}{2}}}\right)\right).$$

This is done so that neighboring points have similar ε. Values σ smaller than the above lead to high frequency oscillations in the estimate of $r(q)$ since ε is then forced to be too small in proportion to $h = \frac{1}{M}$. We always use 2 V-cycles per time step, unless otherwise noted. These parameters produce very consistent results across a wide range of resolutions $64 \leq M \leq 1024$ that we tested, see Figures 7.1–7.5.

The computational time necessary to estimate a single $r(q)$ is $O(M^3)$, and to produce a contour plot with the above resolution of σ is $O(M^5)$.

7.4.1 Discussion

We observed a number of pinning intervals for a few examples of coefficients g. The behavior of $r(q)$ in a neighborhood of the pinning intervals is surprisingly consistent across our computations. Namely, the velocity is pinned to a constant value only along a single critical direction, and far away from the pinning interval the value $r(q)$ is proportional to $|q|$ as in the time-independent case. Moreover, $r(q)$ appears to be only Lipschitz continuous at the points on the relative interior of the pinning interval, see Figure 7.2. For the critical direction, this has a boosting effect for smaller $|q|$ and slowing effect for larger $|q|$ along the pinning interval, compared to the nearby directions. We observed that this leads to an appearance of a stable flat part (facet) of the free boundary in the critical direction, see Figure 7.6.

In the particular case (7.4.1b), there is an indication of the appearance of a whole class of pinning intervals near the main diagonal $(1, 1)$ as a sort of resonance between the pinning intervals in directions $(1, 0)$ and $(0, 1)$, see Figure 7.3. Some of

M	ε^{-1}				
	8	16	32	64	128
64	8.7×10^{-2}	6.3×10^{-2}	5.2×10^{-1}	1.0×10^{0}	1.5×10^{0}
128	5.9×10^{-2}	5.3×10^{-2}	5.9×10^{-2}	3.9×10^{-1}	1.0×10^{0}
256	6.5×10^{-2}	5.8×10^{-2}	2.1×10^{-2}	5.0×10^{-2}	4.0×10^{-1}
512	7.9×10^{-2}	5.7×10^{-2}	2.0×10^{-2}	1.1×10^{-2}	5.9×10^{-2}

TABLE 7.1: The maximum of the error of the numerical estimate of $r(q)$ for $g(x,t) = \sin(2\pi(x_1 + t)) + 2$ as compared to the estimate of $r(q)$ using the ODE method in one dimension described in Section 2.2.2 for $q = (q_1, 0)$, with a small sample of values q_1 away from the ends of the pinning interval $[\frac{1}{3}, 1]$ for various values a parameters M and ε. Our method appears to be first order accurate in M if ε is chosen appropriately.

the level sets in the first quadrant have an appearance of the level set the ℓ^1 norm $\|p\|_1 := |p_1| + |p_2|$, which is a typical example of a so-called crystalline anisotropy. Somewhat surprisingly, no such effect is apparent in the case (7.4.1c) with four traveling waves in the axis directions, see Figure 7.5.

Our estimate of $r(q)$ appears to be first order accurate in M, see Table 7.1, and consistent when changing the resolution and other parameters, see Figure 7.1 and Figure 7.6.

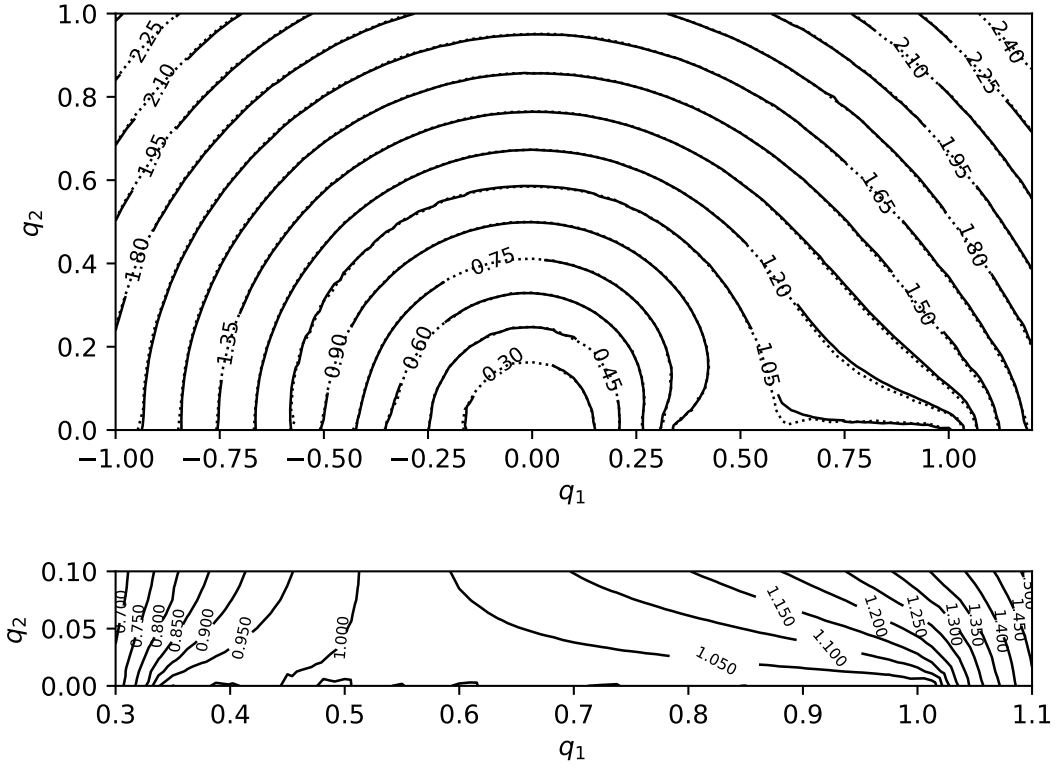

FIGURE 7.1: (Top) The contour plot of $r(q)$ with $g(x,t) = \sin(2\pi(x_1 + t)) + 2$. The pinning interval $[\frac{1}{3}, 1] \times \{0\}$ is apparent, see Lemma 2.2.1, where the average velocity is pinned to 1. The solid contours were obtained with $M = 256$, while the dotted contours were obtained with $M = 128$. (Bottom) Detail of the pinning interval computed with $M = 512$.

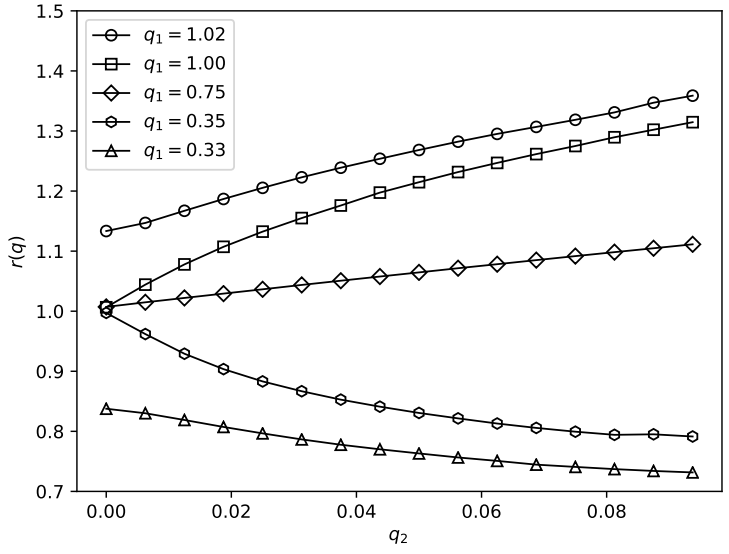

FIGURE 7.2: Values of $r(q)$, $q = (q_1, q_2)$, for $g(x,t) = \sin(2\pi(x + t)) + 2$ with $M = 1024$ as a function of q_2 for several chosen of q_1.

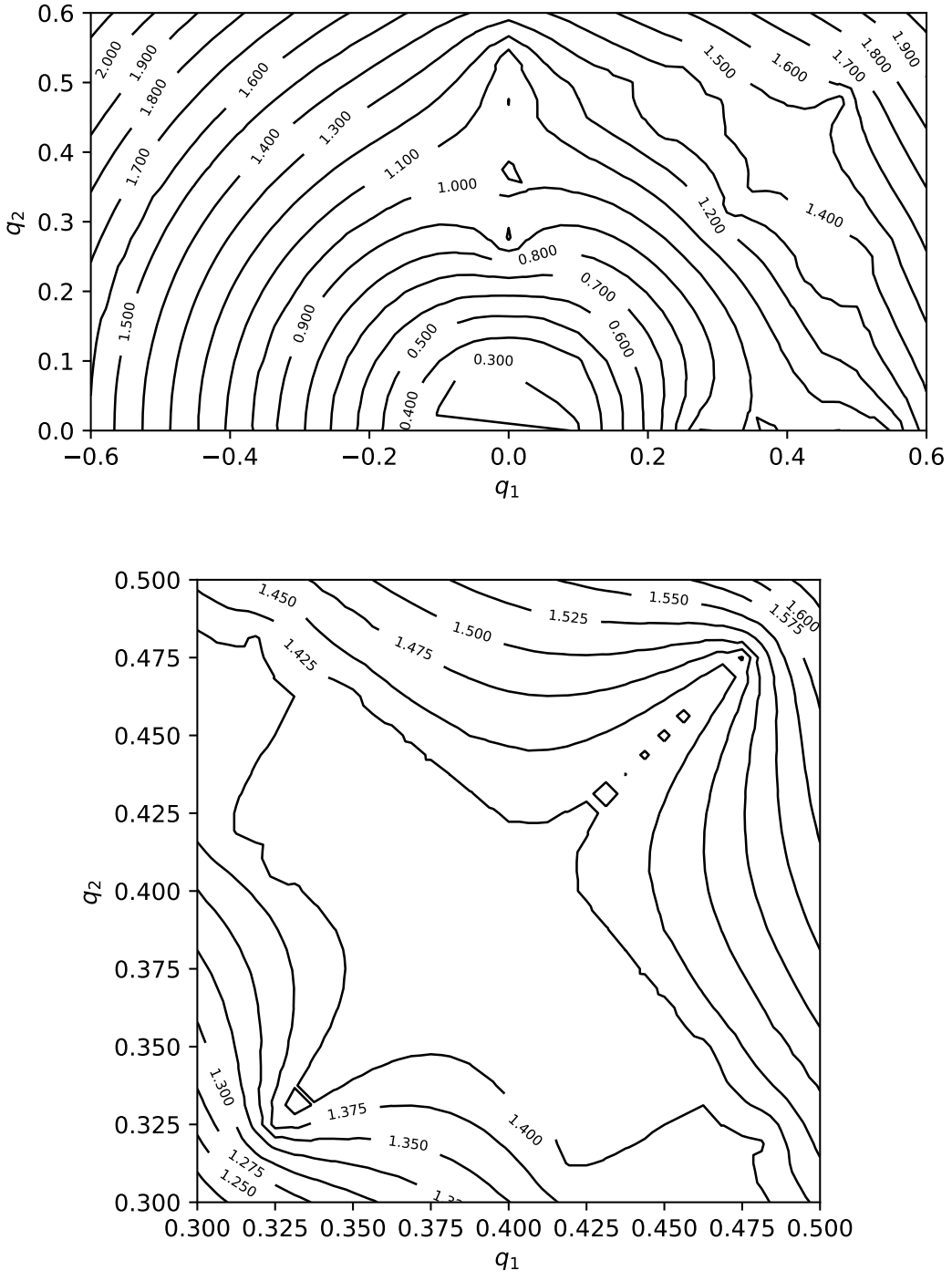

FIGURE 7.3: (Top) Contour plot of $r(q)$ with $g(x,t) = \sin(2\pi(x_1 + t)) + \sin(2\pi(x_2 + t)) + 3$ and $M = 256$. As expected, pinning intervals appear in directions $(1,0)$ and $(0,1)$, however, there is also a visible pinning interval in direction $(1,1)$ where the velocity appears to be pinned to $\sqrt{2}$. The plot is symmetric with respect to the reflection across the direction $(1,1)$. (Bottom) Detail with $M = 1024$ around the pinning interval with velocity $\sqrt{2}$. There might be other pinning intervals nearby. The small squares along the diagonal are artifacts of contour reconstruction.

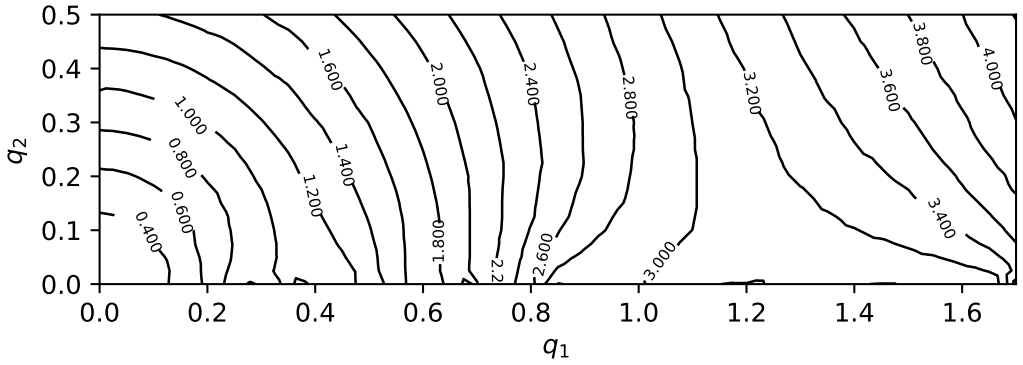

FIGURE 7.4: Contour plot of $r(q)$ with $g(x,t) = \sin(2\pi(x_1 + t)) + \sin(2\pi(x_1 + 3t)) + 3$ computed with $M = 256$. The two visible pinning intervals along the q_1 axis where the velocity is pinned to 1 and 3.

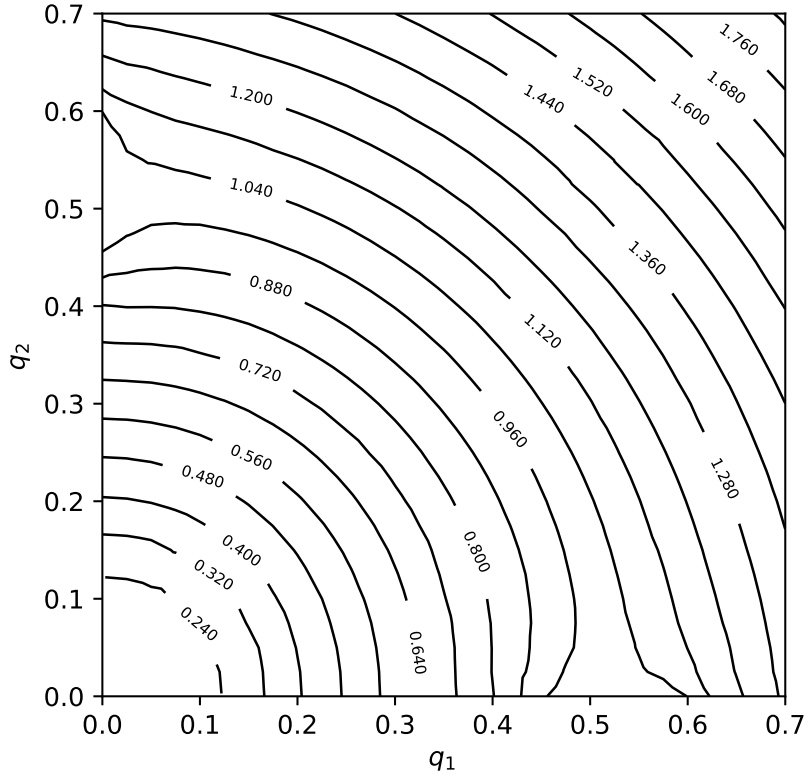

FIGURE 7.5: Contour plot of $r(q)$ with $g(x,t) = \frac{1}{2}\cos(2\pi t)(\sin(2\pi x_1) + \sin(2\pi x_2)) + 2$ with $M = 256$. Pinning intervals appear in the directions of $(1,0)$, $(-1,0)$, $(0,1)$ and $(0,-1)$ (the plot is symmetric with respect to the rotation by $\frac{\pi}{2}$).

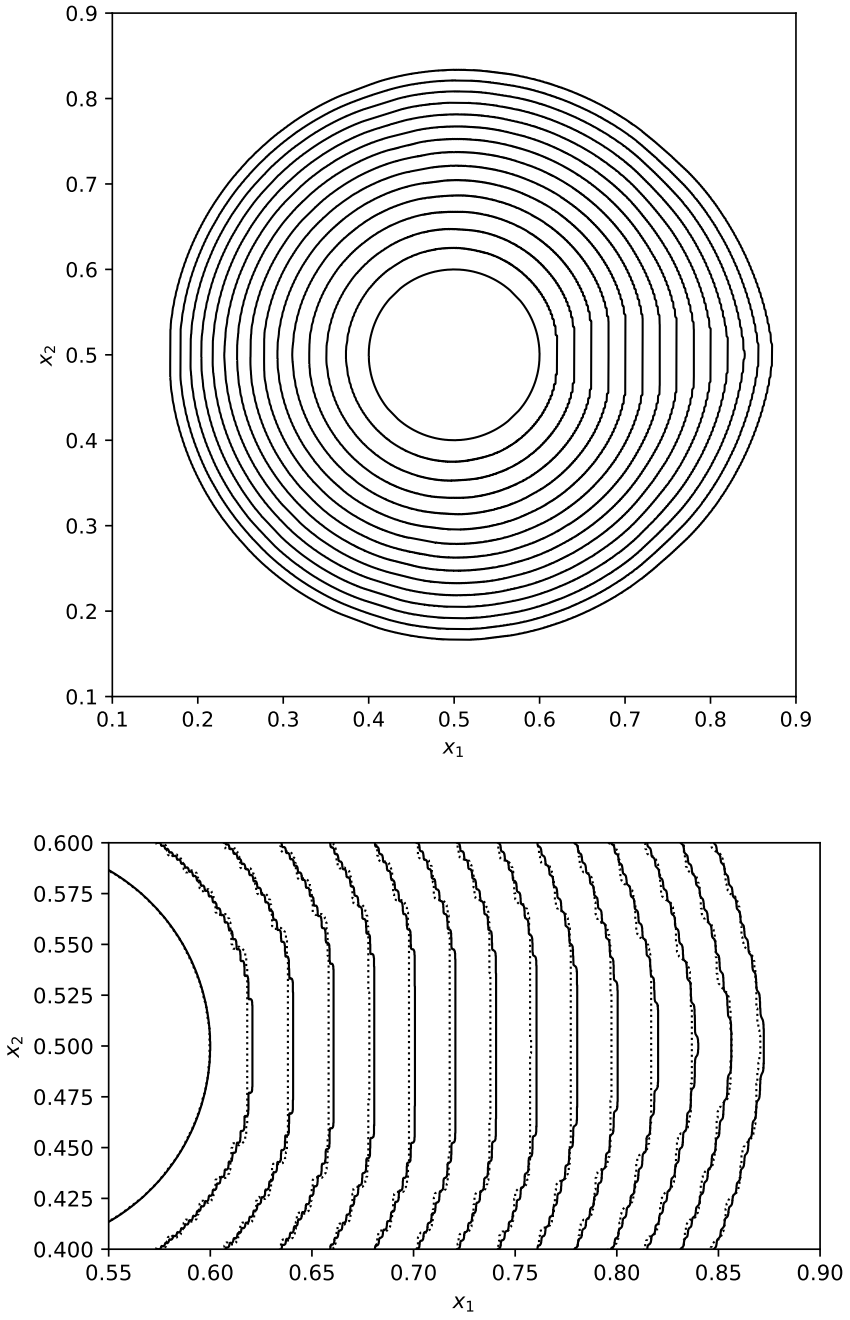

FIGURE 7.6: (Top) The free boundary of the numerical solution of the Hele-Shaw problem with a given source $f = 1500 \max\{0.1 - |x - (\frac{1}{2}, \frac{1}{2})|, 0\}$ and a function $g(x,t) = \sin(2\pi(x_1 + t)) + 1.05$ with initial data $\Omega_0 = \{x : |x - (\frac{1}{2}, \frac{1}{2})| < 0.1\}$. The free boundary is plotted at times $t = 0.02m$, $m \in N$. A facet seems to appear in direction $(1, 0)$. It reaches its maximum length at $t \approx 0.12$. Solid line is the solution with $M = 8192$, $\varepsilon = \frac{1}{512}$, while the dotted line is with $M = 2048$, $\varepsilon = \frac{1}{128}$. We used 1 V-cycle. (Bottom) Detail of the region with facets.

Bibliography

[1] P.G. Saffman and F.R.S. Sir Geoffrey Taylor. The penetration of a fluid into a porous medium or hele-shaw cell containing a more viscous liquid. pages 155 – 174, 1988. doi: https://doi.org/10.1016/B978-0-08-092523-3.50017-4. URL https://www.sciencedirect.com/science/article/pii/B9780080925233500174.

[2] Stanley Richardson. Hele shaw flows with a free boundary produced by the injection of fluid into a narrow channel. *Journal of Fluid Mechanics*, 56(4): 609–618, 1972.

[3] Norbert Požár. Homogenization of the hele-shaw problem in periodic spatiotemporal media. *Arch. Ration. Mech. Anal.*, 217(1):155–230. ISSN 0003-9527. doi: 10.

[4] Irma Palupi and Norbert Požár. An efficient numerical method for estimating the average free boundary velocity in an inhomogeneous hele-shaw problem. *The Science Report of Kanazawa University*, 62, 2018. ISSN 2433040X.

[5] Alan E Berger, H Brézis, and Joel C W Rogers. A numerical method for solving the problem $u_t - \Delta f(u) = 0$. *RAIRO Anal. Numér.*, 13.

[6] Fernando Quirós and Juan Vázquez. Asymptotic convergence of the stefan problem to hele-shaw. *Transactions of the American Mathematical Society*, 353(2):609–634, 2001.

[7] Inwon C. Kim. Homogenization of a hele-shaw problem in periodic and random media. *Arch. Ration. Mech. Anal.*, 194(2):507–530, . ISSN 0003-9527. doi: 10.1007/s00205-008-0161-1.

[8] F.D.A. Aarão Reis, D. Bolster, and V.R. Voller. Anomalous behaviors during infiltration into heterogeneous porous media. *Advances in Water Resources*, 113:180–188, 2018. ISSN 0309-1708. doi: https://doi.org/10.1016/j.advwatres.2018.01.010. URL `http://www.sciencedirect.com/science/article/pii/S0309170817309715`.

[9] L. C. Piccinini. Homogeneization problems for ordinary differential equations. *Rend. Circ. Mat. Palermo (2)*, 27(1):95–112. ISSN 0009-725X. doi: 10.1007/BF02843869.

[10] Inwon Kim. Liquid drops sliding down an inclined plane. *Trans. Amer. Math. Soc.*, 366(11):6119–6150, . ISSN 0002-9947. doi: 10.1090/S0002-9947-2014-06236-3.

[11] H. Ibrahim. On the rate of convergence in periodic homogenization of scalar first-order ordinary differential equations. *SIAM J. Math. Anal.*, 42(5):2155–2176. ISSN 0036-1410. doi: 10.1137/080738830.

[12] A. A. Lacey. Bounds on solutions of one-phase stefan problems. *European J. Appl. Math.*, 6(5):509–516. ISSN 0956-7925. doi: 10.1017/S095679250000200X. Complex analysis and free boundary problems (St. Petersburg, 1994).

[13] Bento Louro. Remarks on the quasisteady one phase stefan problem. *Proc. Roy. Soc. Edinburgh Sect. A*, 102(3-4):263–275. ISSN 0308-2105. doi: 10.1017/S0308210500026354.

[14] Avner Friedman. A one phase stefan problem. *Indiana Univ. Math. J.*, 24 (11):1005–1035. ISSN 0022-2518.

[15] José-Francisco Rodrigues. *Obstacle problems in mathematical physics*, volume 134 of *North-Holland Mathematics Studies*. North-Holland Publishing Co., Amsterdam. ISBN 0-444-70187-7. Notas de Matemática [Mathematical Notes], 114.

[16] L.A. Caffarelli. Continuity of the temperature in the stefan problem. *Indiana Univ. Math. J.*, (28):53–70.

[17] R. E. White. An enthalpy formulation of the stefan problem. 19(6):1129–1157, 1982.

[18] Fernando Quirós and Juan Vázquez. Asymptotic convergence of the stefan problem to hele-shaw. *Transactions of the American Mathematical Society*, 353(2):609–634, 2001.

[19] Hideki Murakawa. A linear scheme to approximate nonlinear cross-diffusion systems. *ESAIM: Mathematical Modelling and Numerical Analysis*, 45(6): 1141–1161, 2011. doi: 10.1051/m2an/2011010.

[20] J. W. Thomas. *Numerical partial differential equations: Conservation laws and elliptic equations*, volume 33 of *Texts in Applied Mathematics*. Springer-Verlag, New York. ISBN 0-387-98346-5. doi: 10.1007/978-1-4612-0569-2.